END
DATE
FILMED
2 -86
DTIC

ARL-SYS-R-34

(12)

AR-003-969

AD-A162 054

DEPARTMENT OF DEFENCE

DEFENCE SCIENCE AND TECHNOLOGY ORGANISATION

AERONAUTICAL RESEARCH LABORATORIES

MELBOURNE, VICTORIA

SYSTEMS REPORT 34

AN OPTIMISATION METHOD FOR RECONSTRUCTION OF FLIGHT PATH TRAJECTORIES FROM NON-SYNCHRONOUS TIME-SAMPLED OBSERVATIONS BY TWO CINE CAMERAS

by

DTIC
ELECTE
DEC 6 1985
B

A. Ross, L. Mockridge and D. Drumm

Approved for Public Release

OCTOBER 1984

85 12 2 147

AR-003-969

DEPARTMENT OF DEFENCE
DEFENCE SCIENCE AND TECHNOLOGY ORGANISATION
AERONAUTICAL RESEARCH LABORATORIES

SYSTEMS REPORT 34

AN OPTIMISATION METHOD FOR
RECONSTRUCTION OF FLIGHT PATH TRAJECTORIES
FROM NON-SYNCHRONOUS TIME-SAMPLED
OBSERVATIONS BY TWO CINE CAMERAS

by

DTIC
ELECTE
DEC 6 1985
B

A. Ross, L. Mockridge and D. Drumm

SUMMARY

Helicopter flight path trajectories in approach to a tactical landing aid were monitored, ad hoc, *by two cine cameras. Post-trial trajectory reconstruction using simple triangulation methods was confounded by the presence of an unknown bias error in the orientation of one camera, and by non-synchronous camera timing. The report describes the concept, formulation and implementation of an optimisation method which pools all data for a trajectory, permits extraction of bias terms, and yields a complete trajectory smoothed in space and time.*

CONTENTS

Dist

A-1

1. INTRODUCTION

Tactical night approach and hover/landing in operational conditions is a particularly difficult phase of flying operations. Various man-portable aids are available for *ad hoc* installation by ground troops to provide visual guidance to the pilot. The quality and value of such aids have been subjects of interest and investigation by ARL staff for a number of years.

During a field exercise, conducted in July 1980, two Boeing CH-47C (Chinook) helicopters operated by No.12 Squadron RAAF made several runs involving approach, near hover, and overshoot at a site where a visual approach aid known as a PLS (Proportional Landing System) had been erected for the purpose. Runs were made by various pilots during late afternoon, dusk, and night conditions.

The exercise was observed and monitored by ARL staff with the aim of assessing, broadly, by comparison with the daylight runs, the quality of the night runs, the existence of any differences in variability between day and night trajectories, and whether difficulties with tactical night approaches by helicopters warranted further attention from ARL.

The trajectories were recorded by *ad hoc* instrumentation assembled hurriedly at short notice. The basic instrumentation took the form of two Kodak K 100 16 mm cine cameras with film transport modified, using d.c. motors and gearboxes, to yield 1/20th second exposures at nominally one-second intervals. One camera viewed the approaches 'head on' from a position looking over the approach aid; the second camera viewed the trajectories 'broadside' from a position several hundred metres off the nominal approach track. The locations of the cameras were determined with respect to geographic landmarks by conventional surveying methods. A full description of the exercise, instrumentation, analysis and conclusions is given in Reference 1.

The objective in using cine camera instrumentation was to permit subsequent reconstruction of the trajectories for detailed analysis, and assessment of flight path control in relation to the guidance information available based on the known characteristics of the visual aid.

Trajectory reconstruction was initiated using triangulation methods on the discrete data obtained from frame by frame analysis of the films. The results were less than satisfactory and indicated several unexpected sources of error. Predominantly there was good evidence that one camera ran at less than the calibrated speed, but considerable uncertainty about whether the speed was stable and constant for all aircraft runs. Secondly, although interpolation methods were used to obtain 'synchronous' data from the two cameras, one set of camera-to-aircraft sight lines lay consistently below those for the other camera; indicating the presence of a camera boresight angular bias, again with uncertainty about its stability.

It was recognised that the initial trajectory reconstructions, although adequate for indicating general trends, were of doubtful accuracy for assessing flight path control vis-à-vis PLS guidance information. For that purpose a more complex analytical procedure was required, and needed to be one which permitted the extraction of bias terms. As such, it would need to use all trajectory data available, at least for any one aircraft run, and preferably for the ensemble of runs.

As far as was (or is) known, no such methodological technique has been documented. Thus more precise reconstruction of the trajectories required the evolution and formulation of an appropriate method. This document deals with the principles underlying, and logical development of, such a technique.

2. GENERAL METHODOLOGY

2.1 The Problem

The problem can be concisely stated as follows: given that two, time-sequenced, non-synchronous cameras were used to observe an aircraft trajectory (i.e. that of a helicopter in an

1

approach to a 'hover'), and that from a frame by frame examination of the exposures, estimates can be obtained of the 'azimuth' and 'elevation' of the target (i.e. the helicopter) relative to each camera—to reconstruct the trajectory in space and time.

There are several sources of potential error. These include:

(a) *systematic errors:*

(i) survey: bias in the true camera locations relative to the assumed locations,

(ii) bore sight: bias in the true camera optical 'centre-line' relative to the assumed centre-line, in azimuth, elevation and roll,

(iii) frame rate: average frame rate of the two cameras relative to one another (and in absolute time if velocity and other time derivatives are to be extracted),

(iv) lens distortion: barrel/pin-cushion distortion of camera and projector lenses,

(b) *random errors:*

(i) stability of camera axes,

(ii) stability of film transport timing in cameras,

(iii) stability of film location in camera and projector,

(iv) resolution in data extraction from individual frames.

The survey was based on conventional triangulation techniques with one base-line length measurement. The set of azimuthal bearings appropriate to each camera location included the camera to camera line and also the lines to several fixed point markers and to a geographical landmark: Samuel Hill. No geographic reference (e.g. North-seeking) was incorporated. Elevation measures were based on the quality of setting-up of the theodolite to a gravity referenced bubble.

Site detail reconstitution and comparison with ordnance survey map data for the area, indicated a high level of accuracy in azimuthal data. Less confidence can be held on elevation data due to uncertainty in referencing (bubble reference) and lack of independent confirmatory data.

The cine cameras were fitted with externally mounted view finders, and not 'through the lens' systems. It must be assumed, therefore, that bias errors in elevation and azimuth are likely. The cameras were set up using bubble referenced beds.

The framing rates of the two cameras were set and calibrated in the laboratory before departure for the trial, and checked on return. One camera appeared to have remained stable but the other had departed significantly from its calibrated speed. Initial analysis of data from film confirmed that the camera had been running slow during the exercise. Any new analytic procedure should seek to indicate the average relative frame rates for each aircraft run because it cannot be assumed that the speed of the 'slow' camera was constant for all runs.

The distortion introduced by the camera and projector lenses can be assumed to be deterministic, so that from calibration processes the data can be corrected. The camera/projector optical laws were calibrated post-trial by, effectively, photographing a suitable large measurable grid and comparing real world dimensions with 'azimuth' and 'elevation' data extracted by the same process as for the trials data. The lenses were, however, assumed to have axial symmetry.

It should be possible to reduce the effects of random errors, to some degree, by smoothing processes. Also by using an appropriately chosen minimisation procedure using parametric

descriptors for biasses and timing rate it should be possible to identify, and thereby extract, those errors. Such a process would require 'pooling' the data over any one trajectory, and if possible, the ensemble of data over all trajectories.

2.2 Methods

Assume, initially, that the exposures from the two cameras are equispaced in time and synchronised. The data would then consist of sets of 4 sample values representing the concurrent observations of azimuth and elevation from each camera. Each successive data set could then be used to obtain one estimate of the position in space of the target. The succession of position estimates represents the trajectory.

At least two different methods, described below, may be used to obtain position estimates.

Method 1

For each camera, a data pair (azimuth, elevation) defines a line in space. The two lines, one from each camera, in general do not intersect. The shortest distance between the two lines corresponds to that of their common perpendicular. One logically based estimate of the aircraft position is the mid-point of that common perpendicular. This estimate may be obtained by a different procedure (but which leads to the same result) as follows: assign parametric values (x, y, z) for the aircraft position, determine the perpendicular distances from (x, y, z) to each skew line, square and sum those distances to form a quadratic error function, then minimise the error function by variation of (x, y, z). The values of (x, y, z) which yield the minimum value of the error function is taken as the 'best' estimate of position.

The minimisation applies to an error function scaled to spatial quantities, $(\delta x, \delta y, \delta z)$, and may be termed minimisation in the spatial domain.

Method 2

An alternative minimisation procedure is as follows: assign parameter values (x, y, z) for the aircraft position; for those values, determine the parameter-dependent values of 'azimuth', ψ, and 'elevation', α, for each camera, equivalent to the 4 values of the data set; form a quadratic error function as the sum of squares of differences; then minimise the error function by variation of the parameters (x, y, z). Again, the 'best' estimate is that set of (x, y, z) values which gives the minimum value of the error function.

In this case the error function is scaled to data quantities, $(\delta \psi_1, \delta \alpha_1, \delta \psi_2, \delta \alpha_2)$, and may be termed minimisation in the data (or 'angles') domain.

The two methods lead to approximately the same result *only* when the target (estimate) is equi-distant from the two cameras. In effect Method 2 gives due allowance for the effect of range. Method 1 weights spatial errors equally, regardless of the difference in range to each camera, and of the dependence on range of the angles subtended.

In consideration of an analytical technique for pooling all data across the entire trajectory to extract bias errors, which is also intended to find a trajectory that 'best fits' the data, it would seem that Method 2 is to be preferred.

The time sequence of estimates of aircraft position (obtained by either method) would not, in general, be 'smooth'. Each position estimate, defined by 3 parameters (x, y, z) is derived from the 4 data values in the data set; the 4th degree of freedom allowing the minimisation, so that each estimated point of the trajectory may be considered to have one degree of freedom associated with it. For many trajectory points it should be possible to incorporate constraints to smooth the trajectory in the minimisation process.

Again by way of example, for discussion, suppose the trajectory were understood (or

3

assumed) to be a straight line constant speed trajectory. Then the complete trajectory could be defined by the 6 parameters:

$$X_0, \; Y_0, \; Z_0, \; \Delta x, \; \Delta y, \; \Delta z$$

defining a sequence of positions:

$$P_i \equiv (X_0 + i\Delta x, \; Y_0 + i\Delta y, \; Z_0 + i\Delta z) \qquad i = 0 \ldots N.$$

The 6 parameters require a minimum of 2 data sets with 8 measured quantities (and thus also 8 degrees of freedom) for the minimisation. In that case the solution for the two-point trajectory would be the same as that obtained by separately estimating one position (each with one degree of freedom) for each data set. For greater numbers of data sets, progressively more degrees of freedom become available to manipulate other parameters that may be assigned (e.g. systematic biasses) and to suppress the effects of random errors.

Where the trajectory is known to be more complex than the simple case taken above, as would be the case for a helicopter approaching the hover, the trajectory is less easily specified parametrically. It may, however, be reasonable to assume that over any short segment (a few seconds) the true trajectory can be adequately modelled, or fitted, by a relatively simple parametric law or equation.

It is useful, at this point, to synthesise a notional trajectory in order to illustrate several other aspects which raise questions about choosing the 'domain' and techniques for smoothing/interpolation.

Consider a straight line trajectory, but with aircraft speed reducing to near zero, thus approximating an approach to a hover. Define the line of the trajectory as:

$$\frac{x}{l} = \frac{y}{m} = \frac{z-h}{n}$$

and set:

$$l : m : n = 1 : 10 : 2$$

depicting an aircraft approaching substantially from the 'y' direction (see Fig. 1) to a hover near $(0, 0, h)$. Synthesising speed decreasing linearly with time, let the sequence of positions be:

i	Δy	y	x	z
1		450	45	100
	--150			
2		300	30	70
	—120			
3		180	18	46
	—90			
4		90	9	28
	—60			
5		30	3	16
	—30			
6		0	0	10

Assign camera locations and sight lines: Camera 1 at $(-280, 200, 0)$ pointing $(1, 0, 0)$ and Camera 2 at $(20, -100, 0)$ pointing $(0, 1, 0)$, so that Camera 1 is observing 'broadside', whilst Camera 2 is observing near 'head-on' with significant changes in range.

4
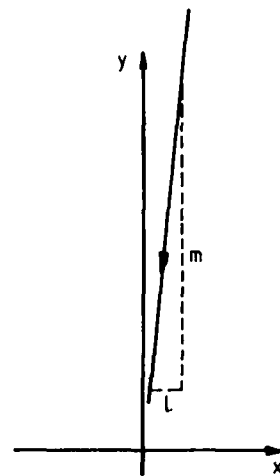
(a) Plan
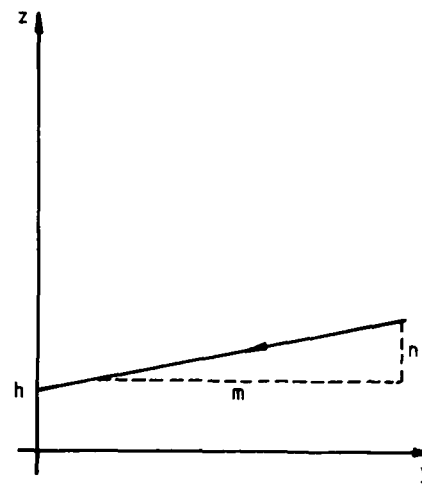
(b) Side elevation
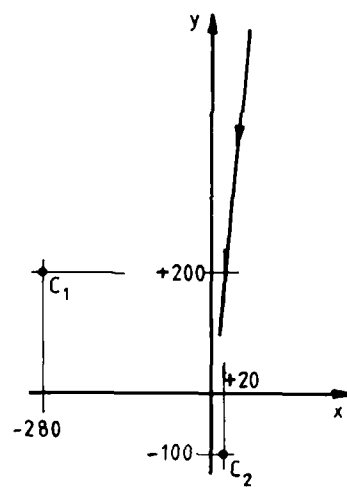
(c) Camera locations

FIG. 1   SYNTHESISED ILLUSTRATIVE TRAJECTORY

Using simplified equations for translation and rotation to camera axes, and optical scaling:

$$x_1 = 200 - y \qquad\qquad x_2 = x - 20$$

$$y_1 = 280 + x \qquad\qquad y_2 = y + 100$$

$$z_1 = z \qquad\qquad z_2 = z$$

$$\psi_1 = 10x_1/y_1 \qquad\qquad \psi_2 = 10x_2/y_2$$

$$\alpha_1 = 10z_1/y_1 \qquad\qquad \alpha_2 = 10z_2/y_2$$

yields the data sets:

i	ψ_1	α_1	ψ_2	α_2
1	−7·6923	3·0769	0·4545	1·8182
2	−3·2258	2·2581	0·2500	1·7500
3	0·6711	1·5436	−0·0714	1·6429
4	3·8062	0·9689	−0·5789	1·4737
5	6·0071	0·5654	−1·3077	1·2308
6	7·1429	0·3571	−2·0000	1·0000

In Figure 2 are plotted the data pairs $(\psi, \alpha)_i$ for the two cameras, which depict the trajectory as seen by the cameras. Both views show the straight line characteristic of the trajectory. Figure 2(a) showing $(\psi, \alpha)_1$ for Camera 1 gives a reasonably faithful representation of the space/time relationships with reducing speed. Figure 2(b) showing $(\psi, \alpha)_2$ for Camera 2 illustrates the effect of changing range and the resulting change of weighting of spatial distances between positions, particularly at short range.

In Figure 3 are plotted the individual values of ψ_1, α_1, ψ_2, α_2 against time. Extending the notional trajectory in time, the hover (zero speed) is achieved at a value of t of 6·5, after which the aircraft would, in this contrived example, retrace the trajectory in the reverse direction. Further, as time tends to infinity the data values tend asymptotically to finite limits:

$$\psi_1 \rightarrow -100$$

$$\alpha_1 \rightarrow 20$$

$$\psi_2 \rightarrow 1$$

$$\alpha_2 \rightarrow 2$$

the last two of which are realistic, whereas the first two are somewhat nebulous.

The important point illustrated by this example is that, despite the straight line nature of the trajectory, the speed change occurring is such that when the data are plotted against time as a master parameter, the shape of the resulting curves are in a form that, in principle, cannot be fitted by polynomials.

Hence, smoothing and interpolation of the separate data sequences $\psi_1(i)$, $\alpha_1(i)$, $\psi_2(i)$, $\alpha_2(i)$ by conventional techniques *before* processing to obtain position estimates would be ill-advised.

The alternative is to apply smoothing to the sequence of noise corrupted position estimates. The position estimates are (at this stage) assumed to be in the form (x, y, z, t) i.e. position at a
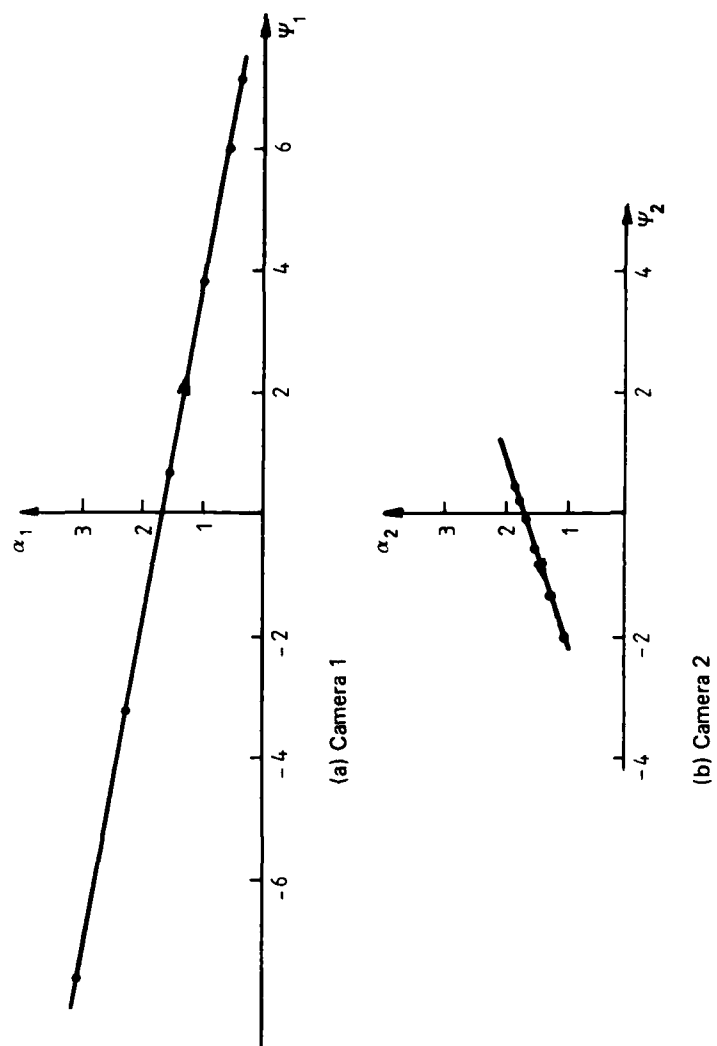
(a) Camera 1

(b) Camera 2

FIG. 2   DATA PAIRS (ψ, α) FOR CAMERAS 1 & 2
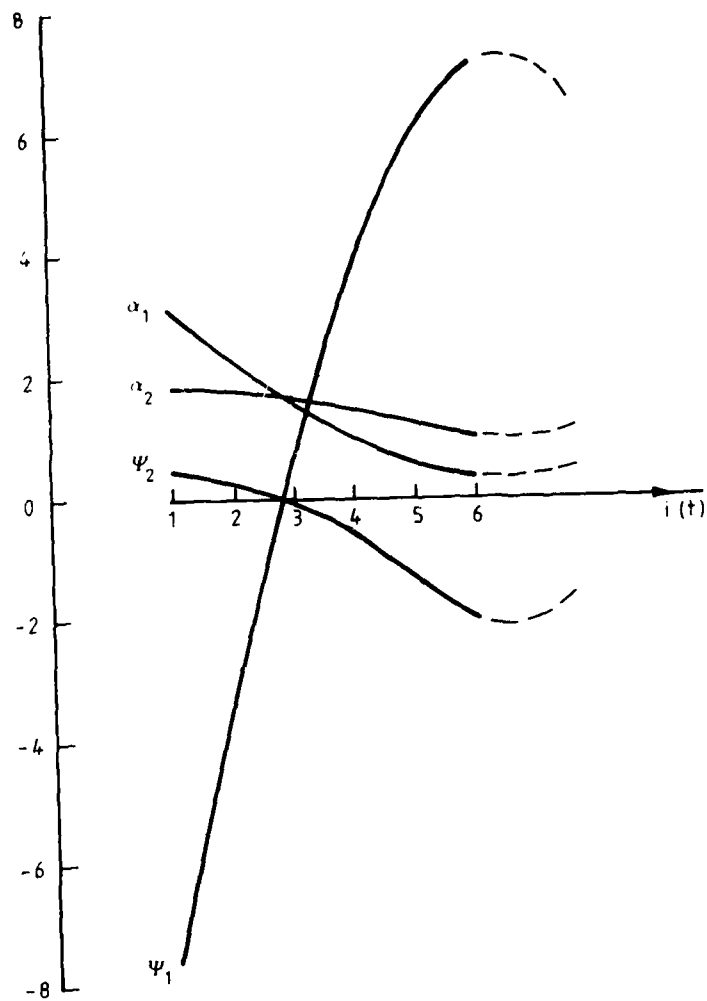
FIG. 3   DATA SETS $(\psi_1, \alpha_1, \psi_2, \alpha_2)$ vs TIME

3

given time—indeed time is the variable by which data from the two cameras are to be meshed. It would be possible to process the estimates without consideration of time, that is, as random samples of positions on the trajectory. The fitting procedure would then take the form of first or higher order regressions between the variables x, y and z. It might then be possible subsequently to reassign 'smoothed' time.

That process would lose much of the space/time relationship that is intrinsic to the original 'raw' position samples. It seems preferable to apply a curve fitting procedure that uses time as a master variable. As such, the procedure would involve the smoothing in time of spatial variables. This could be done as a 'single pass' processing of the position estimates to give the trajectory directly. An alternative approach is to incorporate a fitting procedure as part of an iterative process which progressively refines the 'smoothed' trajectory estimates in a global minimisation routine addressing the entire trajectory. The latter would allow the iterative trade-off of error magnitudes along the trajectory, allow for the time matching of well defined texture or perturbations within local segments of the trajectory, and also allow parametric identification of bias errors common to all parts of the trajectory.

From the point of view of flight control, the pilot would be attempting to achieve a well controlled (straight line?) flight path, with progressively decreasing speed, so that smoothing should not suppress that trend. However, pilot corrections to deviations from the desired flight path will involve curvature in space. The level of smoothing/fitting that should be applied is a matter of judgement.

To fit a straight line, whilst allowing curvature in time (acceleration), requires the acceleration vector to be constrained to be aligned with the velocity vector. Fitting requires 7 degrees of freedom in the assignment of 3 position components, 3 velocity components and 1 acceleration magnitude. To allow for spatial curvature, all 3 components of acceleration need to be assigned so that 9 degrees of freedom are required. This implies that the latter case would yield an exact fit (no smoothing) if the input data consisted of 3 position estimates equispaced in time.

In general, that implication is true, but because each position estimate is itself derived with 1 degree of freedom from a data set of 4 values, the fitting process can be embedded in a minimisation routine in which 9 parameters are searched to fit the 12 initial data values corresponding to 3 data sets.

Whilst that principle appears attractive, its extension to an error function covering the entire trajectory would require the complete trajectory to be modelled/fitted by a set of equations with a limited number of parameters in order for the multi-parameter search to be feasible. So far, that approach has not been useful.

2.3 Strategy Adopted

The broad strategy adopted for development in detail was as follows:

(a) to formulate an iterative procedure which, at each iteration, would revise the 'fitted' trajectory to improve the quality of fit to the experimental data, and overall would (hopefully) converge to a stable solution.

(b) within each iteration:
  (i) each trajectory 'raw' point corresponding to a camera observation would be updated by searching (x, y, z) to minimise a quadratic error function scaled in the 'data domain' and based on both the corresponding 'last smooth' point from the previous iteration and the camera data.
  (ii) smoothing would be by local smoothing, over a span of a few seconds, of 'raw' (x, y, z, t) values and would allow for curvature in space and time.

(c) a gross error function value, applicable to the entire trajectory would be formed by summing, across the trajectory, the residuals (minima) of the individual point error functions.

9

Several potential problems were foreseen and are described below. Some, but not all, were evident in the long run.

The minimisation searches would be local, with revised 'last smooth' points at each iteration. There was, therefore, no guarantee that the gross error function would reduce monotonically at every iteration.

The process would need to be started with some arbitrary 'smooth' trajectory. There was no guarantee that different solutions might not result from different initial conditions.

With point by point minimisations in each iteration the procedure would be computationally expensive, and not particularly efficient.

To extract bias error terms would require them to be assigned parametrically, and for the gross error function asymptotic value (as a function of the parameter set) to be minimised by variation of the values in the parameter set. In other words the iterative procedure described above, which on convergence defines a trajectory, must itself be bedded into a higher level minimisation routine. In view of the potential problems mentioned above it was considered to be unwise to attempt to make that an autonomous process, and preferable that it be operator controlled interactively.

It was also recognised that some of the parameters were likely to be inter-related. For example with evidence that without bias correction one set of camera-to-aircraft sight lines lay consistently below those for the other camera, bias correction could be applied to either camera—but with opposite signs. Also, for the camera viewing broadside, elevation and azimuth adjustments have rather similar effects. It was thought that final judgement of 'quality' of the solution would be likely to be subjective.

What has not been dealt with so far is the question of non-synchronous timing! That can be dealt with by the procedure proposed—in fact, it was evolved in order to do so—but not without some added complication.

Two parameters T_0 and ΔT are assigned, for extraction by the overall minimisation, to define a start time and framing interval of one camera relative to the other. Having been assigned (as bias type parameters) they remain constant over the iteration to convergence, and fix the relative timing of exposures, and hence the meshing of the data leading to that solution.

The local point by point minimisations need, however, to be redefined because data from only one camera is, in general, appropriate to that instant in time. Without a second sight line to give a triangulation 'fix' there is a tendency for the point minimisation to allow the search to drift along the one sight line. This can be overcome by synthesising 'pseudo-data' notionally appropriate to the other camera as those data corresponding to the 'last smooth' point. Such a constraint is weak in that it adaptively follows the solution through the iterations.

Finally there is a housekeeping aspect that must be incorporated into the procedure. In principle the determination of a trajectory is possible only for the period of time for which data from both cameras are available. Thus, having assigned T_0 and ΔT, only the 'overlap' of camera data time spans should be used. The routine must therefore select out the appropriate time meshed data for processing.

3. FORMULATION

3.1 Quadratic Error Function

A central feature of the strategy proposed is the definition of a quadratic error function, scaled in the 'data domain', and suitable both for optimising individual points in space relative to the experimental data and for assessing the global quality of a trajectory fit. In turn, this requires a procedure for transforming the spatial domain parameters (x, y, z) to equivalent 'azimuth' and 'elevation' values $(\psi_1, \alpha_1, \psi_2, \alpha_2)$ for the cameras, based on the site geometry, the assumed bias error parameters, the lens distortion laws, and the camera/projector scalings to the data domain.

3.1.1 Site Geometry

For the purposes of analysis and trajectory reconstruction a reference coordinate system was defined, viz: a right hand system, having its origin at the location of Camera 2 (the 'head-on' camera), z-axis vertical, positive upwards, and y-axis horizontal and aligned with the nominal optical centre-line of Camera 2, itself pointing along the pre-planned approach track.

Referenced to that coordinate system, the site/camera geometry derived from survey data is shown in Figure 4.

To transform the coordinates of an arbitrary point (x, y, z) in the reference frame, defined by:

$$[X]^T = [x, y, z]$$

to coordinates $[X_{C_i}]^T$ appropriate to the frames of observations of the cameras, requires the translations and rotations given by:

$$[X_{B_i}] = [X] - [X_{A_i}]$$

$$[X_{C_i}] = [R(El_i)][R(Az_i)][X_{B_i}]$$

where

$$[X_{A_1}]^T = [-615\cdot4, 327\cdot4, 1\cdot9]$$

$$[X_{A_2}]^T = [0, 0, 0]$$

define the camera locations in the reference frame and

$$[R(Az_i)] = \begin{bmatrix} \text{Cos } Az_i & \text{Sin } Az_i & 0 \\ -\text{Sin } Az_i & \text{Cos } Az_i & 0 \\ 0 & 0 & 1 \end{bmatrix}$$

$$[R(El_i)] = \begin{bmatrix} 1 & 0 & 0 \\ 0 & \text{Cos } El_i & \text{Sin } El_i \\ 0 & -\text{Sin } El_i & \text{Cos } El_i \end{bmatrix}$$

provide the rotations to the camera orientations, where

$$Az_i = As_i + \Delta Az_i$$

$$El_i = Es_i + \Delta El_i$$

are the Euler angles, in the reference frame, of the camera centre lines (optical axes), and from the survey:

$$As_1 = -81\cdot5$$

$$As_2 = 0$$

$$Es_1 = 0$$

$$Es_2 = 0$$

and ΔAz_1, ΔAz_2, ΔEl_1, ΔEl_2 are assignable parameters to synthesise bias errors during interactive processing seeking the global minimum.

11

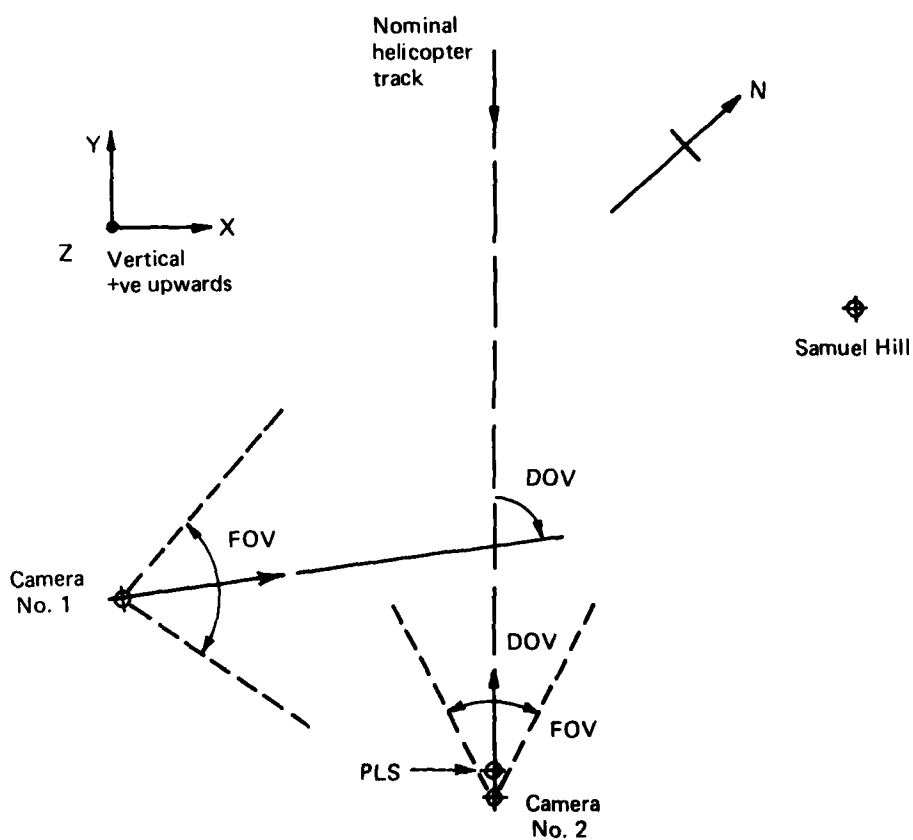|	Coordinates X, Y, Z (m)	Direction of view DOV (deg)	Field of view FOV (deg)
Camera No. 1	−615.4, 327.4, 1.9	81.5	84
Camera No. 2	0.0, 0.0, 0.0	0.0	54
Samuel Hill	621.2, 856.3, 52.3	−	−
PLS	0.0, 39.6, −1.5	−	−

FIG. 4   SITE GEOMETRY (PLAN)

3.1.2 Lens Distortions/Data Scalings

A basic assumption, deemed to be adequate for the purposes of trajectory reconstruction, was that all lenses (camera lenses, wide angle lenses and projector lens) were axially symmetric. Calibration was therefore limited to off-axis (radial) measurements taken in the horizontal plane through the optical centre-lines.

Each camera, in turn, was set up and bubble referenced on a tripod in front of a building with well defined, spaced, vertical pillars. The tripod was positioned accurately in front of a central pillar and adjusted to be symmetrically located with respect to the lateral pillars. A sequence of exposures was taken with the camera pointing firstly at the central pillar, then at 5 degree azimuth increments across a scan equal to the field of view. The azimuth increments were set by vernier control on the tripod moving steadily clockwise and then steadily anticlockwise to check for backlash. The number of angular settings compounded with the number of pillars gave a multiplicity of points of known geometry to facilitate deduction of the calibration laws.

Ray paths from real world objects to images on film involve tangent function relationships in both the real world and camera spaces, and an angular compression law through the wide angle lens/camera lens combination. On projection, similar tangent function relationships hold for the projector space and the final screen space, with a compression/expansion of angles through the projector lens. Final dimensions on the screen (the 'data domain') are directly dependent on the arbitrary distance from projector lens to screen.

Trials data had been extracted by direct reading with the images back projected on to a 1 mm by 1 mm grid, and the field of view covering a lateral span of about ± 180 mm. Readings had been estimated to the nearest $0 \cdot 5$ mm.

Assuming that the camera/lens and projector/lens dimensions and characteristics are reasonably well matched, then the dominant effects should be the tangent function relationships of the real world and screen spaces, and the angle compression law of the wide angle lens. Other effects and mismatches should be secondary. With those assumptions, the plotting of screen image offset distance r_s against real world offset angle θ should yield a relationship of the form:

$$r_s = d_s \tan \{ f(\theta) \}$$

$$\theta = f^{-1} \{ \tan^{-1}(r_s/d_s) \}$$

where d_s is scalarly related to the projector/screen spacing.

It was found possible to fit the calibration data for both cameras, to an unexpectedly high accuracy, by means of the expression:

$$r_s = k_0 \tan \{\theta/k_i\} \qquad i = 1, 2 \text{ (cameras)}$$

$$\theta = k_i \tan^{-1} \{r_s/k_0\}$$

where:

$$k_0 = 456 \text{ for both cameras}$$

$$k_1 = 2 \cdot 1 \text{ for Camera 1: } 84^\circ \text{ FOV}$$

$$k_2 = 1 \cdot 35 \text{ for Camera 2: } 54^\circ \text{ FOV.}$$

Whilst there is a strong and appealing case for drawing further inferences about camera/projector geometry, this would be unwise and unnecessary. It is emphasised that the relationship was obtained by curve fitting, not by model fitting.

Extending to three dimensions, in a camera coordinate system with camera optical axis aligned with the y-axis, the point (x, y, z) lies at an angle offset from the axis given by θ where:

$$\tan \theta = \frac{\{x^2 + z^2\}^{1/2}}{y}.$$

13

Similarly, the corresponding 'azimuth' and 'elevation' values, $(_iu, _iv)$, in the data domain, satisfy:

$$\tan \frac{\theta}{k_i} = \frac{\{_iu^2 + _iv^2\}^{1/2}}{k_3} \qquad i = 1, 2$$

and

$$\frac{_iu}{x} = \frac{_iv}{z} = \frac{\{_iu^2 + _iv^2\}^{1/2}}{\{x^2 + z^2\}^{1/2}} = \frac{_ir_s}{r}.$$

Hence, given (x, y, z) in camera coordinates, the corresponding data domain values $(_iu, _iv)$ are derived, using

$$r = \{x^2 + z^2\}^{1/2}$$

$$\theta = \tan^{-1}\{r/y\}$$

$$_ir_s = k_0 \tan\{\theta/k_i\}$$

$$_iu = (_ir_s/r) x$$

$$_iv = (_ir_s/r) z.$$

3.1.3 Error Function

As postulated previously the iterative procedure will, within each iteration, conduct a minimisation search to update each point corresponding to a camera observation. Those 'raw' points are then 'smoothed' as the last phase of the iteration. The smoothing process injects the time structure of the observations.

The overall objective of the procedure is progressively to draw the 'smoothed' trajectory away from the nominal initialising trajectory towards that time structured solution which best fits the experimental data. It is therefore seen as necessary for the error function to have two distinguishable components: one that reflects differences with respect to the experimental data, and one that reflects the distance between the search point and the corresponding 'last smooth' point. Without the latter the time structure of the observations will not be an integral component of the adaptive process. In order to add the two components the 'spatial' error term requires appropriate rescaling, as described below. The error function is therefore defined to have the form:

$$E_{ij} = w_d \, \varepsilon_{ij} + w_s \, e_{ij}$$

where

$$i = 1, 2 \qquad \text{(cameras)}$$

$$j = 1, 2, \ldots N_i \qquad \text{(relevant observations per camera)}$$

$$w_d + w_s = 1$$

and the weighting coefficients w_d and w_s are introduced for convenient manipulation of the strength of the 'data' error and 'spatial' error terms.

14

In practice, as stated in 2.3, only the 'overlap' of camera data time spans should be used so that, more precisely:

$$j = n_i, \ldots n_i + (N_i' - 1)$$

$$n_i \geqslant 1$$

$$n_i + (N_i' - 1) \leqslant N_i$$

so that of the full set N_i of observations by the ith camera, only the subset n_i to $n_i + (N_i' - 1)$, of size N_i', are used.

An appropriate 'global' error function for the complete trajectory can then be defined as:

$$E = \sum_i \sum_j E_{ij}$$

or perhaps more rigorously in normalised form as:

$$E = \frac{1}{N_1' + N_2'} \sum_{i=1}^{2} \sum_{j=n_i}^{n_i + N_i' - 1} E_{ij}.$$

'Data' Error Term: ϵ

Assume, for the moment, that the cameras had been synchronised. The data set for a particular observation time would then be

$$(\psi_{1j}, \alpha_{1j}, \psi_{2j}, \alpha_{2j}).$$

The corresponding 'last smooth' point and current search point are denoted by:

$$(x_j^*, y_j^*, z_j^*)$$

and

$$(x_j, y_j, z_j)$$

respectively, and the data domain set derived from the latter, by:

$$({}_1u_j, {}_1v_j, {}_2u_j, {}_2v_j)$$

where the leading subscripts denote the camera/geometry/distortion law for derivation of u and v.

The most obvious formulation of a data error term is:

$$\epsilon_j = \{({}_1u_j - \psi_{1j})^2 + ({}_1v_j - \alpha_{1j})^2 + ({}_2u_j - \psi_{2j})^2 + ({}_2v_j - \alpha_{2j})^2\}$$

and this would be adequate for synchronous observations. However, with non-synchronous cameras the experimental data separate into the form of two time inter-meshed sequences of data pairs:

$$(\psi_{1j}, \alpha_{1j}) \qquad\qquad (\psi_{2k}, \alpha_{2k})$$

with corresponding 'search points' (or 'last raw' points):

$$(x_{1j}, y_{1j}, z_{1j}) \qquad\qquad (x_{2k}, y_{2k}, z_{2k})$$

and 'last smooth' points:

$$(x_{1j}{}^*, \; y_{1j}{}^*, \; z_{1j}{}^*) \qquad\qquad (x_{2k}{}^*, \; y_{2k}{}^*, \; z_{2k}{}^*)$$

from which can be derived the data domain sets:

$$({}_1u_{1j}, \; {}_1v_{1j}, \; {}_2u_{1j}, \; {}_2v_{1j}) \qquad\qquad ({}_1u_{2k}, \; {}_1v_{2k}, \; {}_2u_{2k}, \; {}_2v_{2k})$$

and

$$({}_1u_{1j}{}^*, \; {}_1v_{1j}{}^*, \; {}_2u_{1j}{}^*, \; {}_2v_{2j}{}^*) \qquad\qquad ({}_1u_{2k}{}^*, \; {}_1v_{2k}{}^*, \; {}_2u_{2k}{}^*, \; {}_2v_{2k}{}^*).$$

The subsets $({}_1u_{1j}, \; {}_1v_{1j})$ and $({}_2u_{2k}, \; {}_2v_{2k})$ correspond to the experimental data pairs, but $({}_2u_{1j}, \; {}_2v_{1j})$ and $({}_1u_{2k}, \; {}_1v_{2k})$ are appropriate to the 'alternate' camera, for which there are, in general, no synchronous observations and therefore no experimental data pairs.

A point error term of the reduced form:

$$\epsilon_{ab} = \{({}_au_{ab}-\psi_{ab})^2 + ({}_av_{ab}-\alpha_{ab})^2\}$$

$$a = 1, 2$$

$$b = 1, \ldots N_a{}'$$

would be valid, but unsatisfactory. The data pair $(\psi_{ab}, \; \alpha_{ab})$ defines a sight line from one camera only, and thus defines a line in space and not a single point. Minimisation of the error term ϵ_{ab}, as defined above, would allow the search point to drift along (or close to) that sight line without constraint.

What is needed is a pseudo data pair that effectively synthesises a sight line from the 'alternate' camera. It is possible to do this by using the data pair appropriate to either of the corresponding 'last raw' or 'last smooth' points from the previous iteration. By using the 'last raw' point there would still be a tendency to drift by increments at each successive iteration. Using the 'last smooth' point overcomes that problem and also synthesises a sight line consistent with the 'last' smooth trajectory, both in space *and* time structure.

Hence the form of the data error term adopted for Camera 1 data was:

$$\epsilon_{1j} = \{({}_1u_{1j}-\psi_{1j})^2 + ({}_1v_{1j}-\alpha_{1j})^2 + ({}_2u_{1j}-{}_2u_{1j}{}^*)^2 + ({}_2v_{1j}-{}_2v_{1j}{}^*)^2\}.$$

Similarly for Camera 2 data:

$$\epsilon_{2k} = \{({}_1u_{2k}-{}_1u_{2k}{}^*)^2 + ({}_1v_{2k}-{}_1v_{2k}{}^*)^2 + ({}_2u_{2k}-\psi_{2k})^2 + ({}_2v_{2k}-\alpha_{2k})^2\}.$$

'Spatial' Error Term

The real world spatial distance between the current 'search' point and the 'last smooth' point is given by:

$$\{(x_{ij}-x_{ij}{}^*)^2 + (y_{ij}-y_{ij}{}^*)^2 + (z_{ij}-z_{ij}{}^*)^2\}^{1/2}$$

However, this is not expressed in data domain scaling and requires modification to compensate for the effect of range, or distance, from the cameras, and for camera scalings (discussed in 2.2 with respect to Method 1/Method 2 concepts).

16

Linearising the tangent functions in the distortion/scaling relationships (see 3.1.2) and considering one dimension only by setting z equal to zero, yields the scaling between real world dimensions and data dimensions as:

$$r = \{x^2\}^{1/2}$$

$$\theta = r/y$$

$$_tr_s = k_0\{\theta/k_t\}$$

$$_tu = (_tr_s/r)x$$

which reduces to:

$$_tu = \frac{k_0}{k_t}\frac{x}{y}.$$

Note that within this set of expressions x and y are real world values within a camera based coordinate system after translation and rotation from the reference coordinate system. The terms k_0, k_t provide magnitude scaling whilst the division by y provides compensation for range. Whether the y divisor value to be used should be that of the current search point or of the 'last smooth' point is of little consequence because these should be almost the same; what is more important is to compensate for the change of range from about 1000 metres at the commencement of the helicopter approach run, down to tens of metres at the hover.

The form adopted for the spatial error term was, therefore:

$$e_{ij} = \left(\frac{k_0}{k_t\,y_{cij}}\right)^2 \{(x_{ij}-x_{ij}{}^*)^2 + (y_{ij}-y_{ij}{}^*)^2 + (z_{ij}-z_{ij}{}^*)^2\}$$

where subscript c denotes camera coordinate.

It can be argued that the range divisor should be the two dimensional range (ground range) or three dimensional range (slant range) instead of longitudinal range, thus allowing for offsets from the camera centre-line. This is a matter of subjective judgement. It was considered that the differences in reconstructed trajectories would be negligible. The fact that the term chosen was already available from prior calculations influenced the choice.

In retrospect the 'spatial' error term exerts an effect similar to that of the synthesised sight line in the 'data' error term, such that the pseudo data pairs (u^*, v^*) might be thought to be redundant. The effects are not quite the same, and in any case it was envisaged that the weighting coefficients w_1 and w_2 would be varied interactively to speed up the convergence, and to change the relative influence of the two terms.

Thus the error function to be minimised in the point by point searches to update 'raw' points, against the data from Camera 1 was:

$$E_{1j} = w_1\{(_1u_{1j}-\psi_{1j})^2 + (_1v_{1j}-\alpha_{1j})^2 + (_2u_{1j}-_2u_{1j}{}^*)^2 + (_2v_{1j}-_2v_{1j}{}^*)^2\}$$

$$+ w_2\left(\frac{k_0}{k_1\,y_{c1j}}\right)^2 \{(x_{1j}-x_{1j}{}^*)^2 + (y_{1j}-y_{1j}{}^*)^2 + (z_{1j}-z_{1j}{}^*)^2\}.$$

The minimisation parameters are x_{1j}, y_{1j}, z_{1j} and the terms $_1u_{1j}$, $_1v_{1j}$, $_2u_{1j}$, $_2v_{1j}$ and y_{c1j} are functions of those parameters. The terms ψ_{1j}, α_{1j} are the original experimental observations. The terms $x_{1j}{}^*$, $y_{1j}{}^*$, $z_{1j}{}^*$, as 'last smoothed' values, remain constant during the minimisation, as do $_2u_{1j}{}^*$, $_2v_{1j}{}^*$.

For Camera 2 data

$$E_{2k} = w_1\{(_1u_{2k}-_1u_{2k}{}^*)^2 + (_1v_{2k}-_1v_{2k}{}^*)^2 + (_2u_{2k}-\psi_{2k})^2 + (_2v_{2k}-\alpha_{2k})^2\}$$

$$+ w_2\left(\frac{k_0}{k_2\,y_{c2k}}\right)^2 \{(x_{2k}-x_{2k}{}^*)^2 + (y_{2k}-y_{2k}{}^*)^2 + (z_{2k}-z_{2k}{}^*)^2\}.$$

The 'global' error for assessing the solution quality over the total trajectory was obtained by summing all such terms after they had been individually minimised, viz:

$$E = \sum_{j=1}^{N_1'} \underset{(xyz)}{Min}\{E_{1j}\} + \sum_{k=1}^{N_2'} \underset{(xyz)}{Min}\{E_{2k}\}.$$

E has the dimensions of length to the power two, but could be non-dimensionalised. It has no simple interpretation.

The 'global' error E is itself a function of the parameter set (bias terms and timing constants) input to, and held constant during, the convergence to solution. Extraction of an 'optimum' solution requires evaluation of E for a range of values of each parameter in the parameter set in order to determine the particular parameter set giving a minimum value for E. It was considered unwise to attempt to embed this within yet another level of computational processing for several reasons. Firstly the number of iterations required to guarantee convergence to a stable solution was somewhat unknown and likely to be dependent on the complexity of the trajectory (smooth-textured). Secondly convergence of E could not be guaranteed to be monotonic. Thirdly the procedure is computationally intensive and any intuitive shortcuts or judgements would be of value. Finally it was recognised that there would be significant interaction between parameters that would require careful consideration in the interpretation of results. For example simultaneous increases in the elevations of both cameras would result in a vertically biassed trajectory but with little change in the error structure other than a likely increase in the error terms at the extremes of the trajectory.

It was therefore concluded that final extraction of 'optimum' solutions should be conducted interactively so that a better 'feel' could be obtained across the ensemble of solutions.

3.1.4 Expected Value

From the general form of the error function as defined, it is possible to deduce a lower bound to the value of E that could be expected for a 'good' trajectory solution.

The error function is made up of terms of the form:

$$E_{1j} = w_1\{(_1u_{1j} - \psi_{1j})^2 + (_1v_{1j} - \alpha_{1j})^2 + (_2u_{1j} - _2u_{1j}^*)^2 + (_2v_{1j} - _2v_{1j}^*)^2\}$$

$$+ w_2\left(\frac{k_0}{k_1\, y_{c1j}}\right)^2\{(x_{1j} - x_{1j}^*)^2 + (y_{1j} - y_{1j}^*)^2 + (z_{1j} - z_{1j}^*)^2\}$$

corresponding to each camera frame. For a smooth actual flight trajectory and a 'good' reconstructed solution, it can be expected that for a fully converged solution there will be only very small differences between the 'current raw' point and the 'last smooth' point values at each iteration. In that case the elements $(x_{1j} - x_{1j}^*)^2$, $(y_{1j} - y_{1j}^*)^2$, $(z_{1j} - z_{1j}^*)^2$, $(_2u_{1j} - _2u_{1j}^*)^2$ and $(_2v_{1j} - _2v_{1j}^*)^2$ will be negligible. Thus the significant contributors to the error function will be:

$$E_{1j} \simeq w_1\{(_1u_{1j} - \psi_{1j})^2 + (_1v_{1j} - \alpha_{1j})^2\}.$$

If, further, it is assumed that all systematic bias has been removed, and that the residual dominant random contributions are those arising from the quantising at the data extraction level (i.e. in film reading to the nearest $0.5\,\text{mm}$ on projection) then both $(_1u_{1j} - \psi_{1j})$ and $(_1v_{1j} - \alpha_{1j})$ can be taken to be random samples from a distribution that is uniform between $\pm 0.25\,\text{mm}$, with variance approximately equal to 0.02.

With N_1' and N_2' data pairs (ψ, α) from Camera 1 and Camera 2 respectively in the solution, and a weighting value w_1 equal to 0.5, the expected value of the error function would be:

$$0.5\,(N_1' + N_2')\{2(0.02)\}.$$

18

This sets a lower bound on what might reasonably be expected as a value for the error function when a 'good' solution has been found. In practice it was found that difference terms with values greater than 1.0 occurred, indicating a probable data extraction or transcription error. Such errors were allowed to remain and were not corrected in the experimental data listings.

For the specific case examined in detail later in this report the value of $(N_1' + N_2')$ is approximately 125, leading to a lower bound of 2.5 for the error function. In practice, values close to 4.0 were achieved.

3.2 Minimisation

The requirements for point by point minimisation of each individual error term $E_{ij}(xyz)$ were seen to be quite conventional, and such that a standard software package or library routine could be used. However, the general purpose packages are themselves all iterative and structured to seek an absolute minimum.

In the case in hand it is intended that the 'last smooth' point, on which the error function is dependent, change from iteration to iteration in the process of convergence on the solution trajectory. Again in view of the extent of computation it was decided to limit the minimisation at each iteration to that of a single direction, steepest descent, approximation.

3.2.1 Steepest Descent

In general a minimisation can be initiated from an arbitrary starting point but if limited, as proposed, to only one direction then it should be commenced at each iteration, from the 'last raw' point from the previous iteration.

Commencement of the entire procedure must necessarily be somewhat arbitrary and the initialising 'last raw' points were set equal to the initialising 'last smooth' points derived by time interpolation of a nominal initialising trajectory. For interactive incrementing of parameters in the parameter set, initiation from the 'last raw' points from the previous convergence to solution shortens the subsequent convergence, provided the timing parameters have not been changed. If timing parameters have been changed then the best estimates for starting can be obtained for the non-reference camera by re-interpolating the previous solution trajectory points appropriate to the reference camera.

The steepest descent vector direction is derived directly from the single dimension derivatives at the search commencement point. Because it is intended to iterate convergently into a minimum, it is necessary to estimate derivatives by first differencing of forward and backward steps, hence:

$$E = E(x, y, z)$$

$$E_{x+} = E(x+\Delta, y, z)$$

$$E_{x-} = E(x-\Delta, y, z) \qquad \text{etc.}$$

where step size Δ is prescribed

$$\Delta E_x = E_{x+} - E_{x-} \qquad \text{etc.}$$

so that

$$\frac{\partial E}{\partial x} \simeq \frac{\Delta E_x}{2\Delta} \qquad \text{etc.}$$

19

Defining a 'normalising' divisor as

$$\nabla = \{(\Delta E_x)^2 + (\Delta E_y)^2 + (\Delta E_z)^2\}^{1/2} \neq 0$$

$$l = \Delta E_x/\nabla$$

$$m = \Delta E_y/\nabla$$

$$n = \Delta E_z/\nabla$$

where l, m and n are the direction cosines of the unit vector whose components are proportional to the local derivatives. Step size Δ along that vector direction, towards the minimum, has components:

$$\Delta x = -l\Delta = -\left(\frac{\Delta E_x}{\nabla}\right)\Delta \qquad \text{etc.}$$

If the search point is at the minimum, then:

$$\Delta E_x = 0 = \Delta E_y = \Delta E_z = \nabla$$

leading to a divide by zero. To guard against this ∇ was tested, and if zero the direction cosines were declared as:

$$l = m = 0, \qquad n = 1$$

in order to proceed with a check search in the z direction. That direction was chosen because, in principle, the experimental data (ψ_1, α_1, ψ_2, α_2) yields *primary* redundancy in the height dimension.

Step size Δ is prescribed, and must be chosen small enough to give reasonable estimates of local derivatives, but not so small as to give rise to truncation problems in differencing. Also, as the basic unit for search stepping, its magnitude tends to control resolution. Δ was therefore held as a member of the parameter set, for interactive manipulation. In general a value of $0 \cdot 125$ metre was used.

3.2.2 Stepping

To speed up the search process a coarse technique of step size doubling was used to encompass the minimum (along one vector direction) within a span of three points having two equal spacings, thus permitting quadratic interpolation. Hence:

$$E_{(0)} = E(x_0, y_0, z_0)$$

$$E_{(1)} = E(x_0 + \Delta x, y_0 + \Delta y, z_0 + \Delta z)$$

$$(x_0 + 2\Delta x) = 2(x_0 + \Delta x) - x_0 \qquad \text{etc.}$$

$$E_{(2)} = E(x_0 + 2\Delta x, y_0 + 2\Delta y, z_0 + 2\Delta z).$$

If $E_{(2)} \leq E_{(1)}$, such that the minimum has not been passed, then abandon $E_{(1)}$ and repeat the process

$$(x_0 + 2n\Delta x) = 2(x_0 + n\Delta x) - x_0$$

$$E_{(2n)} = E(x_0 + 2n\Delta x, y_0 + 2n\Delta x, z_0 + 2n\Delta z)$$

20

until $E_{(2n)} > E_{(n)}$, giving

$$E_{(0)} = E(x_0, y_0, z_0)$$

$$E_{(n)} = E(x_0 + n\Delta x, y_0 + n\Delta y, z_0 + n\Delta z)$$

$$E_{(2n)} = E(x_0 + 2n\Delta x, y_0 + 2n\Delta y, z_0 + 2n\Delta z)$$

at equal spacing encompassing the minimum.

3.2.3 Estimation

Given the values $E_{(0)}$, $E_{(n)}$, $E_{(2n)}$, estimates can then be made of the value of the minimum E, and its (x, y, z) location. Quadratic estimation is based on the following:

$$E = E_{(0)} + as + bs^2$$

$$E_{(n)} = E_{(0)} + a + b$$

$$E_{(2n)} = E_{(0)} + 2a + 4b$$

$$\frac{\partial E}{\partial s} = a + 2bs$$

$$= 0 \quad \text{when} \quad s = -a/2b$$

where s is a length parameter in the vector direction corresponding to step size $n\Delta$, then:

$$\frac{a}{2b} = \frac{\{3E_{(0)} - 4E_{(n)} + E_{(2n)}\}}{2\{E_{(0)} - 2E_{(n)} + E_{(2n)}\}}$$

$$c, \text{ say} \qquad 0 \leqslant c \leqslant 2.$$

The estimated location of the minimum is:

$$(x_0 + cn\Delta x, y_0 + cn\Delta y, z_0 + cn\Delta z)$$

the coordinates of which can be obtained from those of the last step:

$$(x_0 + 2n\Delta x, y_0 + 2n\Delta y, z_0 + 2n\Delta z)$$

by:

$$\{x_0 + cn\Delta x\} = \{(x_0 + 2n\Delta x) - x_0\}c/2 + x_0 \qquad \text{etc.}$$

The corresponding value of the error function may then be either estimated from the quadratic fit through:

$$E_{\min]\text{est}} = E_{(0)} + ac + bc^2$$

or calculated through the error function sub-routine using the (x, y, z) coordinates. The latter method was chosen, partly for convenience, partly to avoid truncation problems, but predominantly to avoid mal-estimation in the event of the error function not being well fitted by a quadratic.

21

3.3 Smoothing

As stated previously, the intention is to apply a curve fitting procedure, that uses time as a master variable, to subsets of the 'raw' points derived through the point by point minimisations. This will be a single pass processing at each iteration.

3.3.1 Subsets

The curve fitting procedure was conceived to be, basically, a central estimator process, i.e. given a sequence of values

$$\ldots \; x_{n-2}, \; x_{n-1}, \; x_n, \; x_{n+1}, \; x_{n+2}, \; x_{n+3} \; \ldots$$

then a smoothed value x_n^*, corresponding to x_n, is derived from the central value x_n and its adjacent neighbours x_{n-1}, x_{n+1} and x_{n-2}, x_{n+2} etc. Thus the smoothing is achieved by processing a subset of the sequence having x_n as the central value. This can be done for all values other than those at the extreme ends, which must rely on extrapolation using derivatives.

For the case in hand, where two sequences having different timing are to be time meshed, the process envisaged was to derive the smoothed value x_{1n}^* corresponding to x_{1n} from

$$x_{1,n}$$

$$x_{1,n-1}, x_{1,n+1} \qquad \text{etc.}$$

and

$$x_{2,m}$$

$$x_{2,m-1}, x_{2,m+1} \qquad \text{etc.}$$

where $x_{2,m}$ is the member of the sequence $\{x_{2,k}\}$ closest in time to $x_{1,n}$ (and conversely for $x_{2,n}^*$). The time meshing of the two sequences is such that the subset for processing will involve unequal *time intervals between points in time order.*

3.3.2 Curve Fitting

Several factors influence the choice of a curve fitting routine; the two dominant factors being the span of time (points) to be used in the central estimator, and the degree of complexity of curve model being fitted. The smaller the time span, the fewer the number of degrees of freedom available for model fitting and smoothing. The more complex the model, the greater the number of degrees of freedom required for fitting and hence the fewer available for smoothing.

A subset of 3 points from each camera, 6 points in all, covering some 2–3 seconds of real time, involves 6 input data pairs providing 12 degrees of freedom. Extending the subset to 5 points from each camera, covering 4–5 seconds, provides 20 degrees of freedom.

To fit a straight line constant speed trajectory model (linear in time and space) requires 6 degrees of freedom. To allow for curvature in time only (acceleration along the straight line path) requires 7 degrees of freedom. A constant speed trajectory with spatial curvature (acceleration vector orthogonal to the velocity vector) requires 8 degrees of freedom. Full allowance for curvature in time and space to second order requires 9 degrees of freedom.

The simple linear (time and space) model, fitted to a subset of 6 points, provides a reasonable match of degrees of freedom between curve fitting and smoothing. It is also computationally simple. However, with speed reduction expected in the approach to hover it is obviously not an ideal model.

Extending the model to include speed change along the straight line path (Appendix 1) yields a set of relationships which are more difficult to handle than those of the further extension to full curvature. In the latter case the x, y and z variables separate, with resulting simplification.

The basis of the curve fitting adopted was the assumption that the x, y and z components of the trajectory could, over short segments, be fitted by second order polynomials with time as the independent variable, viz.:

$$x = x_0 + u_x(t - t_0) + a_x(t - t_0)^2 \qquad \text{etc.}$$

The classical least-squares approach to solving for x_0, u_x, a_x etc. yields the solution form:

$$
\begin{bmatrix}
\sum_i 1 & \sum_i (t_i - t_0) & \sum_i (t_i - t_0)^2 \\
\sum_i (t_i - t_0) & \sum_i (t_i - t_0)^2 & \sum_i (t_i - t_0)^3 \\
\sum_i (t_i - t_0)^2 & \sum_i (t_i - t_0)^3 & \sum_i (t_i - t_0)^4
\end{bmatrix}
\begin{bmatrix}
x_0 \\
u_x \\
a_x
\end{bmatrix}
=
\begin{bmatrix}
\sum_i x_i \\
\sum_i x_i(t_i - t_0) \\
\sum_i x_i(t_i - t_0)^2
\end{bmatrix}
$$

where the summation extends over the chosen subset of (t_i, x_i).

The subset chosen, in the subscript notation of Section 3.3.1, was

$$x_{1,n-2}, \; x_{1,n-1}, \; x_{1,n}, \; x_{1,n+1}, \; x_{1,n+2}$$

together with

$$x_{2,m-2}, \; x_{2,m-1}, \; x_{2,m}, \; x_{2,m+1}, \; x_{2,m+2}$$

and their corresponding times, t_i, to determine the smoothed value $x_{1,n}^*$ corresponding to $x_{1,n}$.

A position estimate (x^*, y^*, z^*) is thus obtained corresponding to each camera observation (ψ_i, α_i). Adjacent estimates are strongly correlated through the smoothing, but correlation does not extend beyond five seconds so that the texture of the trajectory is not suppressed.

3.4 Quality of Fit

Assuming that the interactive iterative procedure is convergent to a unique solution—a fitted trajectory—then the quality of that solution needs to be appraised to see how well it fits the original experimental data. Appraisal is also needed through the interactive process in order to decide how next to increment the parameter set, in search of the absolute minimum.

A 'solution', final or intermediate, yields position estimates corresponding to each camera observation, and for each position estimate there is a pair of data domain values (u, v) corresponding to the experimental data pairs (ψ, α). The differences between the experimental and fitted values are closely related to the 'data' error terms of the error function, but the error function uses differences based on the 'raw' search points rather than the corresponding 'smoothed' points. Nevertheless, it is reasonable to assume that the final solution which minimises the error function should be one for which all systematic errors have been compensated, leaving only random errors having distributions with zero means.

The sequence of differences between $(\psi, \alpha)_{ij}$ and $(u, v)_{ij}$ values will indicate any residual uncorrected trends, e.g. all positive values $(\alpha - v)$ for one camera and all negative for the other would indicate a significant elevation error. For the final solution one would like to see an absence

of bias at any portion of the trajectory. The ends of the trajectory can be expected to be particularly *sensitive*.

Apart from the signs and magnitudes of individual difference terms, the means and standard deviations of the sets of differences $\delta\psi_1$, $\delta\alpha_1$, $\delta\psi_2$, $\delta\alpha_2$ provide a measure of the overall quality of the solution.

To assist with parameter incrementing decisions in the interactive process, the program used was structured to provide, after the desired number of iterations, the values for:

Sum of errors: $$\sum_{ij} E_{ij}$$

the error function value,

Maximum error: (i, j), E_{ij}
the location and value of the largest individual error term,

Total number of points: $N_1' + N_2'$
the number of solution points/camera frames being used,

Mean error: $$\frac{1}{N_1' + N_2'} \sum_{ij} E_{ij}$$

together with the four values:

$$\sum_{j=1}^{N_1'} (\delta\psi)_{ij}, \qquad \sum_{j=1}^{N_2'} (\delta\alpha)_{ij} \qquad i = 1, 2.$$

These values facilitate the decisions on which parameters to increment for the next iterations.

On exit from the program a complete solution is required together with the values of the parameter set and data on the residual distribution of errors. The exit listing consisted of:

(a) for each camera:

$j, t_j, x_j^*, y_j^*, z_j^*, \psi_j, \alpha_j, \delta\psi_j, \delta\alpha_j, \qquad j = 1, \ldots N_i'$

and the moments of the residual differences

$$\sum_{j=1}^{N_i'} (\delta\psi_j)^n, \qquad \sum_{j=1}^{N_i'} (\delta\alpha_j)^n \qquad \text{for} \qquad n = 1, 2, 3, 4$$

(b) the error data:
Sum of errors
Maximum error
Number of points
Mean Error

(c) the parameter set leading to that solution:

$T_0, \Delta T, \Delta Az_1, \Delta El_1, \Delta Az_2, \Delta El_2, w_x.$

24

4. IMPLEMENTATION

In this section the trials data and trajectory reconstruction for one helicopter approach are examined in some detail in order to exhibit the nature of the original problem, the operation of the optimisation routine, and the interactive manipulation of the parameter set.

4.1 Trials Data

The particular set of trials data to be dealt with is that which is identified in Reference 1 as "Rockhampton 15".

The raw data, i.e. the 'azimuth' and 'elevation' values measured from the cine film, frame by frame, projections, are given in Table 1. Although the data are listed by frame number, it should not be assumed that the data is 'matched' between cameras. In fact a cursory examination of the elevation values shows that the 'hover' is in the region of Frame No. 69 for Camera 1 and Frame No. 52 for Camera 2.

The plots of Camera 1 and Camera 2 data, depicting the 'views' as seen from those cameras, are given in Figures 5(a) and 5(b). The troughs and peaks in the 'head-on' view can be subjectively matched to phases in the 'broadside' view. The optimisation routine is intended to provide a rigorous method of searching out the optimum match.

In passing, it is of interest to note that the initial parts of the views suggest that an approach was being made to a point well short of the landing aid, at relatively low speed. It is probable that pilot recognition of ground-based textural features (trees?) provided the cue to correct judgement of orientation and height.

4.2 Central Plane Projections

The nominal approach path is in the plane $x = 0$, which corresponds to zero azimuth for Camera 2, the head-on camera. The raw data from Camera 1 implicitly define a set of sight lines to the aircraft from that camera. Those sight lines will intersect the central plane, $x = 0$, in a sequence of points $(o, {}_1y_i, {}_1z_i)$ whose coordinates then define a sequence of elevation values, ${}_2v_{1j}$, appropriate to Camera 2, but not necessarily in time correspondence with the raw data α_{2k} for Camera 2. However, plots of the sequence of elevation values, α_{2k} from Camera 2 and the sequence of elevation values ${}_2v_{1j}$ inferred from Camera 1 may be compared to gain an insight into the relative timing relationship between the two cameras.

The equations for deriving the ${}_2v_{1j}$ values are given in Appendix 2. The resulting plots, of elevation values (in mm) against frame number are shown in Figure 6.

4.3 Relative Timing

The 'character' of the plots in Figure 6 are relatively well matched, but show that Camera 2 ($\times$ symbol) ran slower than Camera 1 ($+$ symbol). This is consistent with the post-trial calibrations of the cameras, which indicated that Camera 1 had maintained calibration but that Camera 2 was running slow.

Comparison of magnitudes of elevation values for the early frame numbers, and rough matching of the troughs and peaks, suggest timing correspondence between

Camera 1	Frame No.	4	46	59	68
Camera 2	Frame No.	1	35	47	52

as plotted in Figure 7.

25

TABLE 1
Rockhampton 15; Raw data from film

Frame No.	Camera 1 Azimuth (mm)	Camera 1 Elevation (mm)	Camera 2 Azimuth (mm)	Camera 2 Elevation (mm)
1	−160·0	60·5	−17·0	74·0
2	−156·0	59·5	−16·5	73·5
3	−152·0	58·5	−15·5	73·0
4	−147·5	57·0	−14·0	72·0
5	−143·5	55·5	−13·0	71·5
6	−139·5	54·0	−12·0	70·0
7	−134·5	52·5	−11·5	67·0
8	−130·5	51·0	−10·5	65·0
9	−126·5	49·5	−9·5	63·0
10	−123·5	48·0	−9·0	61·0
11	−119·0	46·5	−8·0	59·0
12	−115·0	45·0	−7·5	57·0
13	−111·5	43·0	−7·0	54·5
14	−107·5	41·0	−7·0	52·0
15	−103·5	39·0	−7·0	49·5
16	−99·5	37·5	−6·5	48·0
17	−96·0	36·0	−6·5	46·0
18	−92·5	34·5	−6·5	44·0
19	−89·5	33·0	−6·5	41·5
20	−86·5	31·5	−6·0	39·5
21	−83·0	30·0	−5·5	38·0
22	−80·0	28·5	−5·5	36·0
23	−76·5	27·0	−5·5	35·0
24	−73·5	25·5	−5·5	34·0
25	−70·5	24·5	−5·5	32·0
26	−67·5	23·5	−5·0	32·0
27	−64·5	22·0	−5·0	31·0
28	−61·5	21·0	−5·0	30·5
29	−59·0	20·0	−5·0	30·5
30	−56·5	19·0	−5·5	28·5
31	−54·0	18·0	−5·5	28·0
32	−51·5	17·0	−5·5	27·5
33	−49·0	16·5	−5·5	27·0
34	−47·0	16·5	−5·5	26·0
35	−44·5	16·0	−5·5	26·0
36	−42·0	15·5	−5·0	27·0
37	−40·0	15·0	−5·0	27·5
38	−38·0	14·5	−4·5	29·5
39	−35·5	13·5	−3·5	31·0
40	−32·5	13·0	−2·5	32·5
41	−30·0	12·5	−1·5	34·0
42	−26·5	12·5	−0·5	35·5
43	−23·5	12·0	0·5	37·0
44	−20·0	11·5	1·5	28·5
45	−16·0	11·0	3·0	40·0
46	−12·0	10·5	4·0	41·0
47	−7·5	10·5	6·0	42·0
48	−2·5	10·5	8·0	42·0
49	2·5	10·5	10·5	41·5
50	8·0	11·0	13·0	40·0
51	13·0	11·0	16·0	38·0
52	18·5	11·0	19·0	35·5
53	24·0	11·0	22·0	36·0
54	30·0	10·5	25·0	42·0
55	35·5	10·5	—	—
56	41·5	10·5	—	—
57	47·0	10·0	—	—
58	52·5	9·5	—	—
59	57·5	9·5	—	—
60	63·0	8·5	—	—
61	67·5	8·0	—	—
62	72·5	7·5	—	—
63	77·0	6·5	—	—
64	81·0	6·0	—	—
65	85·0	5·0	—	—
66	89·5	4·5	—	—
67	93·0	4·0	—	—
68	97·0	3·5	—	—
69	101·5	3·5	—	—
70	105·0	3·5	—	—
71	109·0	4·0	—	—
72	112·5	5·5	—	—
73	117·0	7·5	—	—
74	121·0	9·5	—	—
75	125·0	12·0	—	—
76	129·0	15·5	—	—
77	133·0	17·0	—	—

26

(a) Camera 1: 'Broadside' view
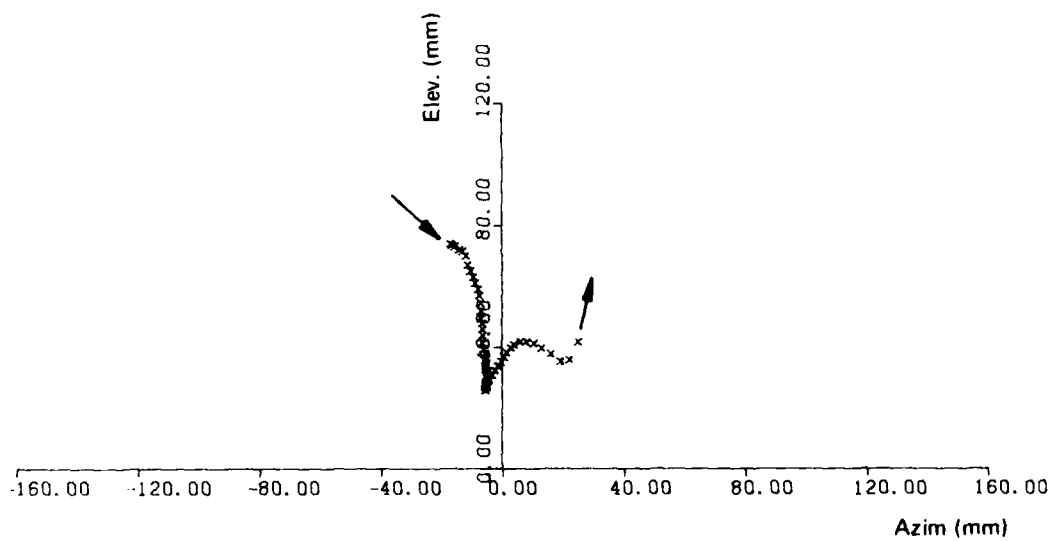
(b) Camera 2: 'Head-on' view

FIG. 5   ROCKHAMPTON 15 'ELEV' vs 'AZIM'

Elevation
(mm)

90.00

80.00

70.00

60.00

50.00

40.00

30.00

20.00

10.00

0.0

47   48

59

52

35

46

68

× (α_{2k}) from Camera 2

+ $(_2V_{ij})$ from Camera 1

0.00   10.00   20.00   30.00   40.00   50.00   60.00   70.00   80.00

Frame No.
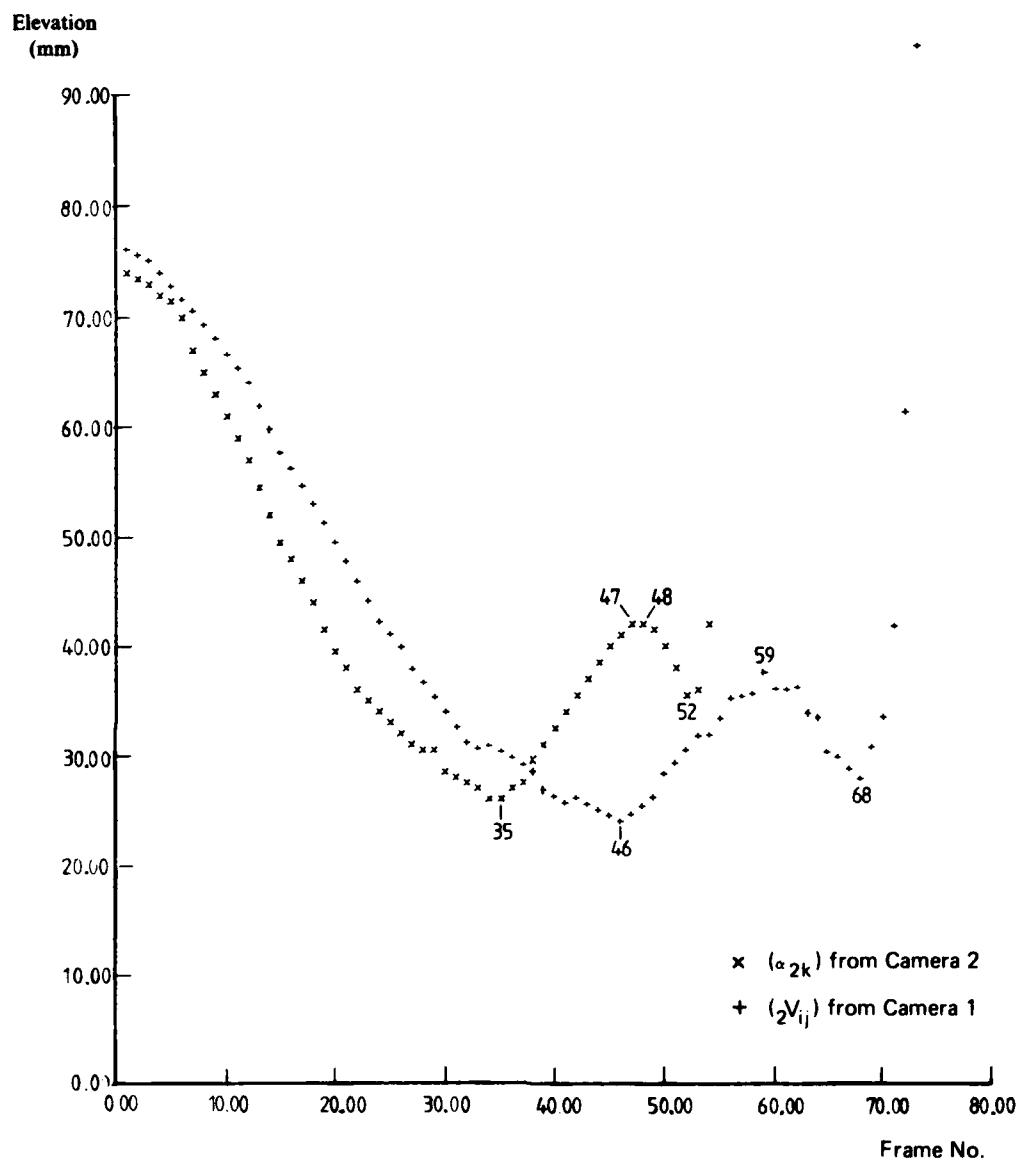
FIG. 6   'TIME' PLOTS OF (α_{2k}) AND CENTRAL PLANE PROJECTIONS $(_2V_{ij})$
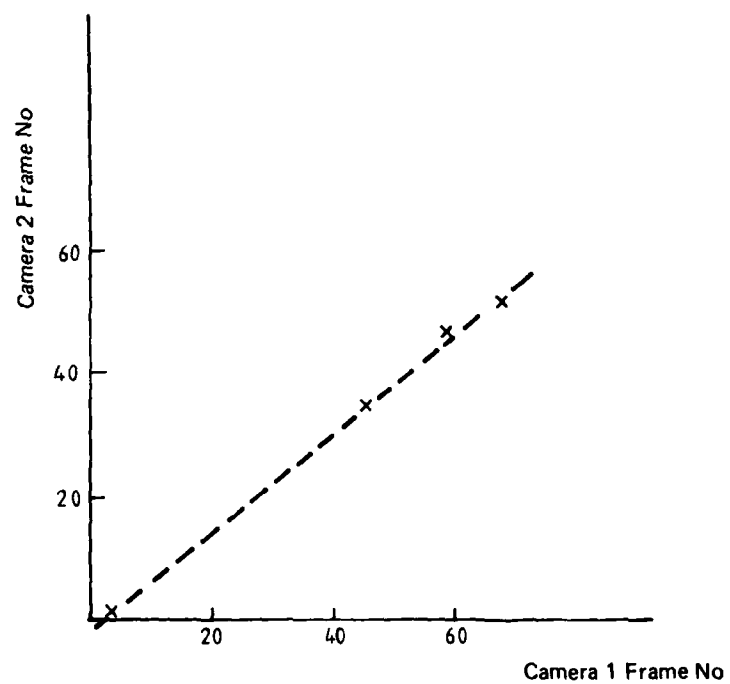
FIG. 7   TIMING CORRESPONDENCE BETWEEN CAMERAS

29

Using Camera 1 timing as the 'master' timing, the times of Camera 2 exposures can be expressed in the form

$$t_{2,n} = T_0 + n\,\Delta T$$

where $t_{2,n}$ is the time of exposure of the nth frame of Camera 2. Based on Figure 7, parameter values suitable for commencing the optimisation search are:

$$T_0 = 3$$
$$\Delta T = 1 \cdot 25.$$

4.4 Trajectory Initialisation

To commence the iterative optimisation procedure requires notional initial values to be assigned as 'last raw' values; 'last smooth' values are derived within the procedure.

A nominal straight line trajectory is used for initialising, by assigning end points to correspond with the data span for Camera 1. The end points used were the same for all trajectories, viz:

$$P_{1I} = (0, 1000, 200)$$
$$P_{1N} = (0, 100, 15)$$

where P_{1I} and P_{1N} correspond to the first and last frames of Camera 1. The full set of Camera 1 values are then derived by direct interpolation (equivalent to a constant speed trajectory) and the Camera 2 values by interpolating on the basis of T_0 and ΔT.

The initialising values correspond to commencing the approach on the centre line 2000 metres out, at 200 metres in height, and descending at constant speed to a point on the centre line, 100 metres from Camera 2 (approximate location of the PLS) at a height of 15 metres.

The possibility that a convergence solution might be dependent on the chosen initialising trajectory was tested by using different initialising end points. In each such case the solution appeared to be completely independent of the initialisation. The P_{1I}, P_{1N} values given above were then adopted as standard for all trajectory reconstructions.

4.5 Iteration Convergence

On entry into the procedure the value of the error function found after the first iteration will be predominantly dependent on the mismatch between the initialising trajectory values and the actual trajectory values. From Figure 5(a) and Figure 6 it is apparent that Camera 1 data includes the final overshoot after completion of the approach. There will therefore be a significant error function value over the first few iterations.

Entering the procedure with values in the parameter set:

T_0	3	time origin of Camera 2
ΔT	1·25	frame interval of Camera 2
w_s	0·5	weighting factor of error function
ΔAz_1	0	azimuth bias, Camera 1
ΔEl_1	0	elevation bias, Camera 1
ΔAz_2	0	azimuth bias, Camera 2
ΔEl_2	0	elevation bias, Camera 2

30

gave an error function value in excess of 16 000 at the first iteration, with rapid convergence (as shown in Figure 8) to less than 80 after 20 iterations and asymptotically to approximately 66·5.

Varying the weighting factor w_s, and thereby varying the relative weighting given to 'spatial' and 'data' error terms did not appear to offer significant improvement in the speed of convergence. A value of 0·5 was therefore adopted and held constant.

4.6 Parameter Search

4.6.1 $(T_0, \Delta T)$ Scan

The timing parameters $(T_0, \Delta T)$ will obviously exert a major influence on the quality of fit. Also there should be a strong interaction between them in that as ΔT is increased the time span of Camera 2 data will be increased, requiring a compensatory change in T_0 to 'centralise' the data with respect to Camera 1 data timing. With 54 observations (frames) from Camera 2 an increase of 0·01 second in ΔT increases the time span of Camera 2 data by 0·54 second, and would require a change of $-0·27$ second in T_0 to recentralise.

A bivariate scan of $(T_0, \Delta T)$ starting at $(3·0, 1·25)$ and incrementing by $(\pm 1·0, \pm 0·01)$ searching for reduction in the error function, yielded the values given in Table 2. For an interactive search it would not be necessary to scan the full array. It is given here for illustrative purposes.

TABLE 2

Results from search scan of $(T_0, \Delta T)$ at $(\Delta Az_1, \Delta El_1, \Delta Az_2, \Delta El_2) \equiv (0, 0, 0, 0)$

T_0 (second)	ΔT (second)	Sum Errors	Maximum Error		No. of Points	Mean Error
			Loc.	Value		
3	1·25	66·57	2, 6	2·17	122	0·55
3	1·26	72·62	2, 6	2·29	123	0·59
3	1·27	79·01	2, 6	2·42	123	0·64
3	1·28	93·99	1, 70	8·81	124	0·76
2	1·25	38·17	2, 6	1·27	122	0·31
2	1·26	40·31	2, 6	1·34	123	0·33
2	1·27	43·40	2, 6	1·41	123	0·35
2	1·28	48·17	2, 6	1·49	124	0·39
1	1·25	24·90	1, 68	1·29	122	0·20
1	1·26	25·09	1, 69	1·15	123	0·20
1	1·27	25·07	1, 64	0·95	123	0·20
1	1·28	48·17	2, 6	1·49	124	0·39
0	1·25	26·59	1, 68	2·15	122	0·22
0	1·26	24·82	1, 69	1·97	123	0·20
0	1·27	21·81	1, 69	1·21	123	0·18
0	1·28	20·64	1, 70	1·05	124	0·17
-1	1·25	43·21	1, 67	2·18	121	0·36
-1	1·26	39·78	1, 68	3·11	122	0·33
-1	1·27	33·67	1, 68	2·02	122	0·28
-1	1·28	30·42	1, 69	1·83	123	0·25

Note that the total number of points being fitted changes systematically as the overlapped time span of data changes. Also the maximum individual error term switches between the early part (2,6) of the trajectory and the 'last' point e.g. (1, 68). The 'last' point appears to provide the maximum error in most cases and the adjustment of time span of Camera 2 progressively brings in extra points from Camera 1 with the clear correlation:
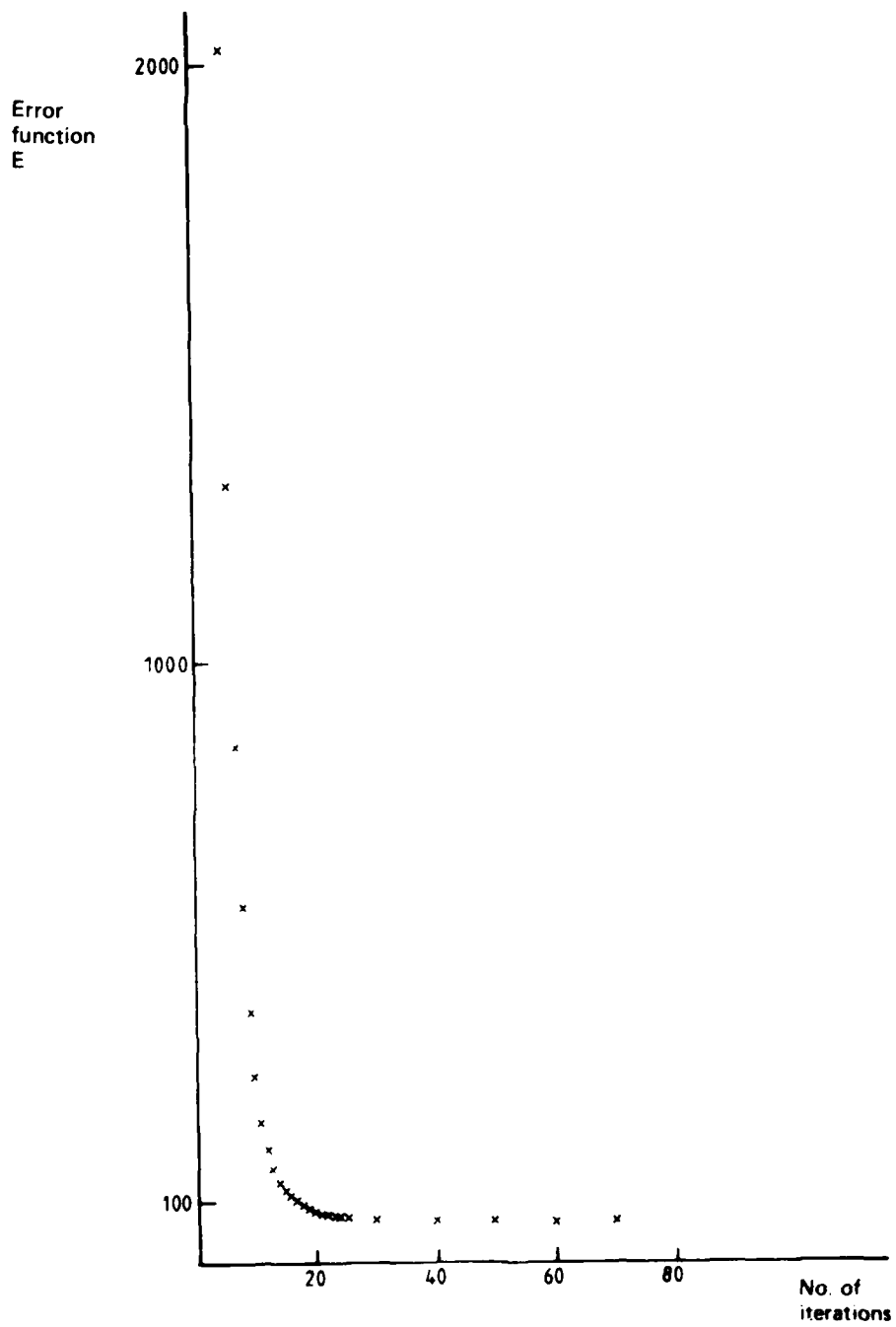
FIG. 8   CONVERGENCE OF ITERATIVE PROCEDURE

32

121 points, maximum error term (1, 67)

122 points, maximum error term (1, 68)

123 points, maximum error term (1, 69)

124 points, maximum error term (1, 70).

We must therefore, expect some discontinuity in the error function.

In array form, the bivariate scan yielded error function values at 100 iterations:

T_0 \\ ΔT	1·25	1·26	1·27	1·28
-1·0	43·21	39·78	33·67	30·42
0	26·59	24·82	21·81	20·64
1·0	24·90	25·09	25·07	25·86
2·0	38·17	40·31	43·40	48·17
3·0	66·57	72·62	79·01	93·99

Plots of error function value against T_0, as loci of constant ΔT are given in Figure 9, and against ΔT as loci of constant T_0 in Figure 10. A bivariate quadratic surface corresponding to the full array is shown in contour form in Figure 11. It must be remembered that this does not necessarily indicate the absolute minimum of the hypersurface.

The major axis of the elliptic contours indicates the interdependence between T_0 and ΔT as predicted, but not quite in the ratio expected. The approximate slope of the major axis is

$$0\cdot01 \text{ second } (\Delta T) \leftrightharpoons -0\cdot2 \text{ second } (T_0).$$

The point $(T_0, \Delta T) = (0, 1\cdot28)$ is close to the centre of the contours, and is a reasonable starting point from which to examine other parameter changes. For those values of $(T_0, \Delta T)$ the sums of data domain differences, viz:

$$\Sigma (\delta \alpha_1) = +32$$

$$\Sigma (\delta \alpha_2) = -24$$

$$\Sigma (\delta \psi_1) = 3\cdot7$$

$$\Sigma (\delta \psi_2) = 1\cdot6$$

indicate a significant bias in elevation, but are inconclusive with respect to azimuth.

4.6.2 $(\Delta El_1, \Delta El_2)$ Scan

With a priori indications that an elevation error existed on one of the cameras, it is illustrative to examine the effects, and interactions, of perturbations of both cameras. If elevation errors of equal magnitude and sign are introduced into both cameras then the relative spatial relation between the two skew sight lines at about mid-trajectory is largely preserved. The spatial relation changes significantly, however, at the ends of the trajectory due to the effects of ranges from cameras, with the hover point end being most sensitive. A strong correlation can be expected.

33

Error
function
E

100 —

90 —

80 —

70 —

60 —

50 —

40 —

30 —

20 —

10 —

ΔT = 1.28

ΔT = 1.27

ΔT = 1.26

ΔT = 1.25

-1   0   1   2   3

To (sec)
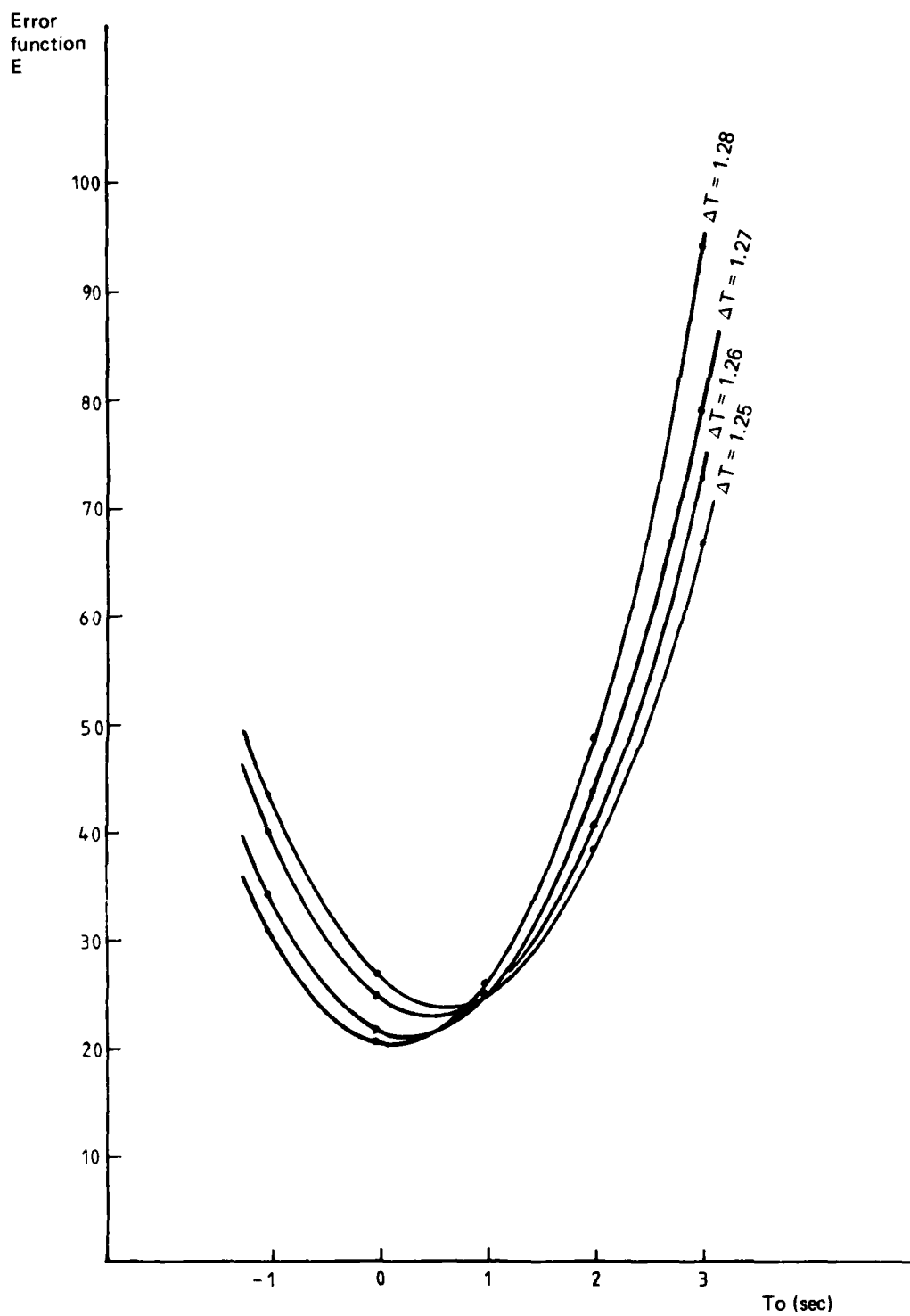
FIG. 9   (To, ΔT) SCAN: E (To) FOR FIXED ΔT

34

FIG. 10   (To, ΔT) SCAN: E (ΔT) FOR FIXED To

35
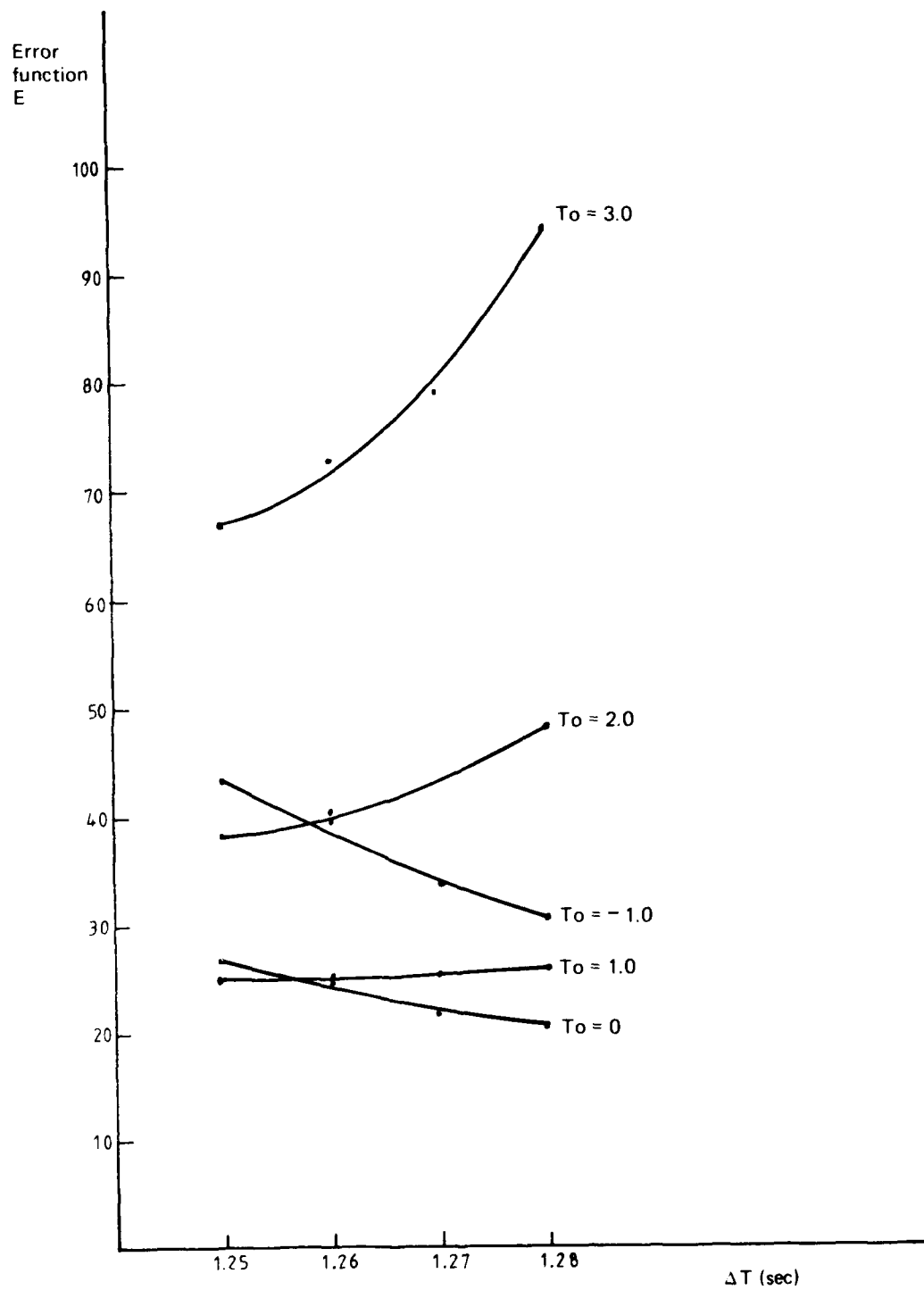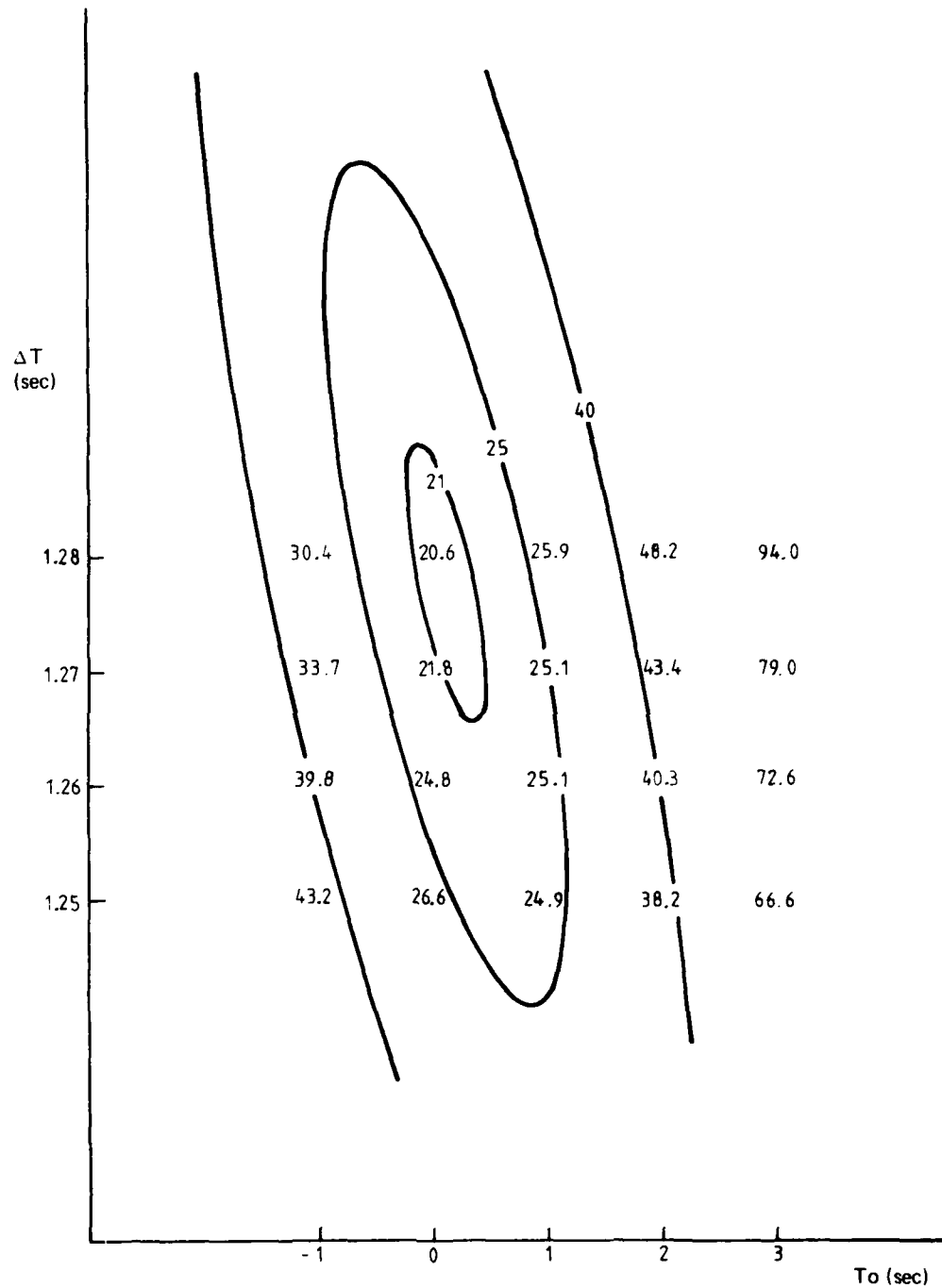
FIG. 11 (To, ΔT) SCAN: QUADRATIC SURFACE CONTOURS

56

Holding $(T_0, \Delta T)$ at $(0, 1\cdot28)$, a bivariate scan of $(\Delta El_1, \Delta El_2)$ starting at $(0, 0)$ and incrementing by $(\pm0\cdot1, \pm0\cdot1)$ degrees yielded the following array of error function values at 50 iterations:

ΔEl_1 \ ΔEl_2	$-0\cdot3$	$-0\cdot2$	$-0\cdot1$	0
0	19·27	15·84	16·88	21·32
$+0\cdot1$	22·06	15·34	11·94	12·04
$+0\cdot2$	31·25	20·02	12·62	9·14
$+0\cdot3$	45·59	30·40	19·09	11·22

With no changes in time meshing the same number of points, 124, was involved in each case. The maximum individual error varied between (1, 1), (2, 15) and (1, 70); and was at (1, 70) in most cases.

Plots of error function value against ΔEl_1, as loci of constant ΔEl_2, are given in Figure 12, and against ΔEl_2, as loci of constant ΔEl_1, in Figure 13. Bivariate quadratic surface contours are shown in Figure 14.

As predicted, a strong interdependence is apparent. A differential bias of about $0\cdot25$ degrees is indicated but it is not clear at this stage which camera has the bias error; or whether errors exist in both. Again it would be unwise to infer too much before examining other parameters. The smallest value of error function found so far corresponds to $(\Delta El_1, \Delta El_2) = (0\cdot2, 0)$ for which the data domain difference sums are:

$$\Sigma(\delta\alpha_1) = 0\cdot019$$

$$\Sigma(\delta\alpha_2) = 4\cdot1$$

$$\Sigma(\delta\psi_1) = 1\cdot7$$

$$\Sigma(\delta\psi_2) = 0\cdot95$$

with no clearcut indication of residual bias errors.

4.6.3 $(\Delta Az_1, \Delta Az_2)$ Scan

Although there is no clear evidence of any azimuth bias, an azimuth scan was included for completeness and illustration. Holding $(T_0, \Delta T, \Delta El_1, \Delta El_2)$ at $(0, 1\cdot28, 0\cdot2, 0)$ a bivariate scan of $(\Delta Az_1, \Delta Az_2)$ starting at $(0, 0)$ and incrementing by $(\pm0\cdot5, \pm0\cdot5)$ degrees to 50 iterations yielded the results given in Table 3. The array of error function values is:

ΔAz_1 \ ΔAz_2	$-0\cdot5$	0	$+0\cdot5$	$+1\cdot0$	$+1\cdot5$
$-1\cdot0$	12·71	10·20	8·34	7·02	6·28
$-0\cdot5$	10·72	8·81	7·86	6·83	7·22
0	10·65	9·14	8·48	8·10	10·97
$+0\cdot5$	11·29	14·53	10·20	11·45	12·45
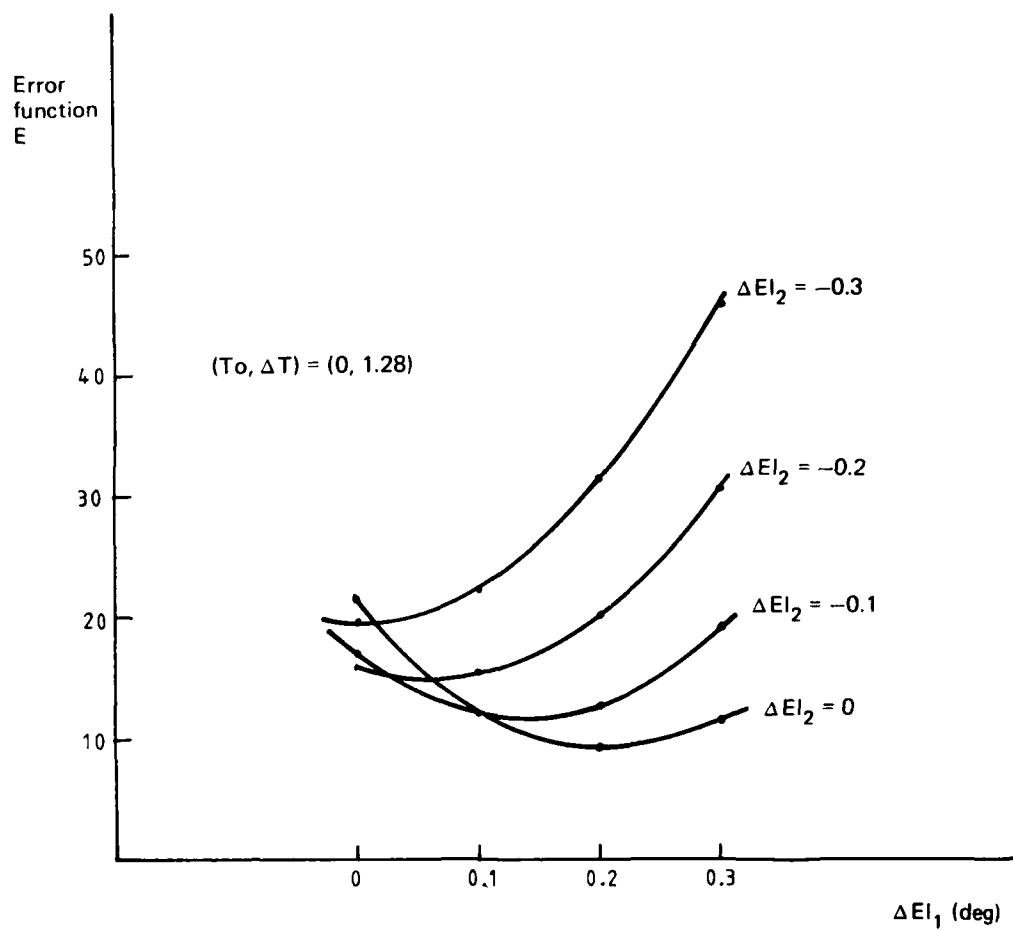
Error function E

$\Delta El_2 = -0.3$

$(To, \Delta T) = (0, 1.28)$

$\Delta El_2 = -0.2$

$\Delta El_2 = -0.1$

$\Delta El_2 = 0$

ΔEl_1 (deg)

FIG. 12 $(\Delta El_1, \Delta El_2)$ SCAN: E (ΔEl_1) FOR FIXED ΔEl_2

Error
function
E

$\Delta EI_1 = 0.3$

$(To, \Delta T) = (0, 1.28)$

$\Delta EI_1 = 0.2$

$\Delta EI_1 = 0.1$

$\Delta EI_1 = 0$

50

40

30

20

10

−0.3   −0.2   −0.1   0

ΔEI_2 (deg)

FIG. 13 (ΔEI_1, ΔEI_2) SCAN: E(ΔEI_2) FOR FIXED ΔEI_1

39
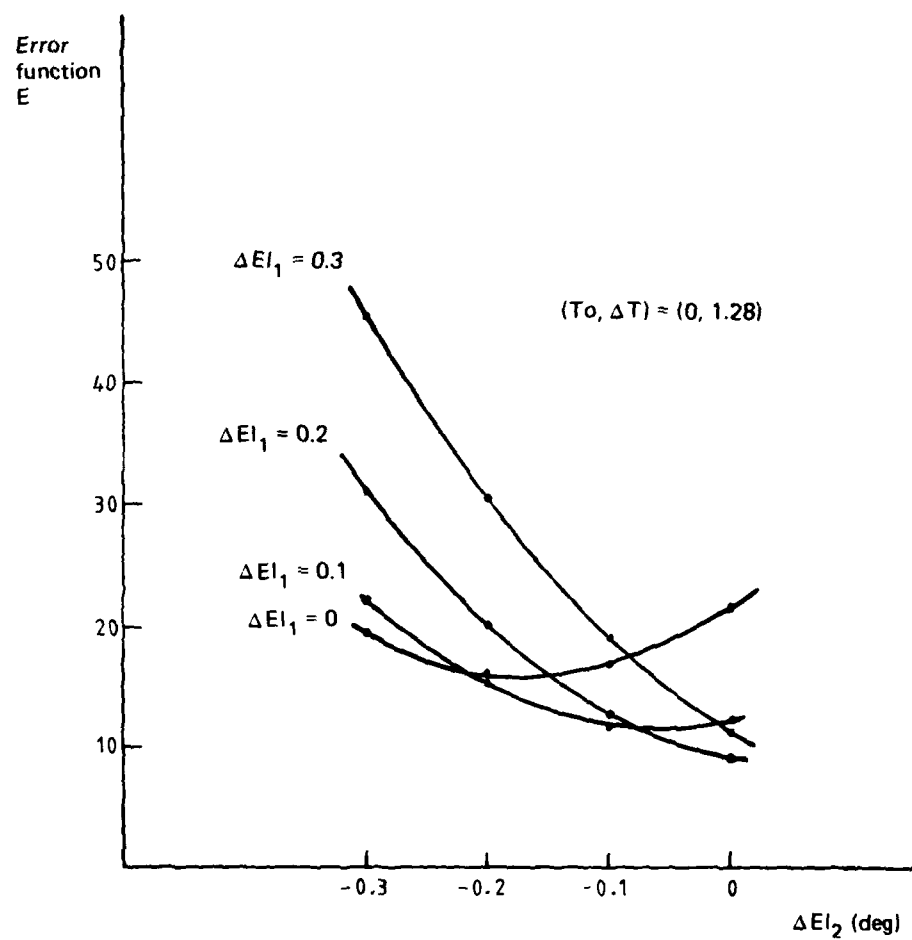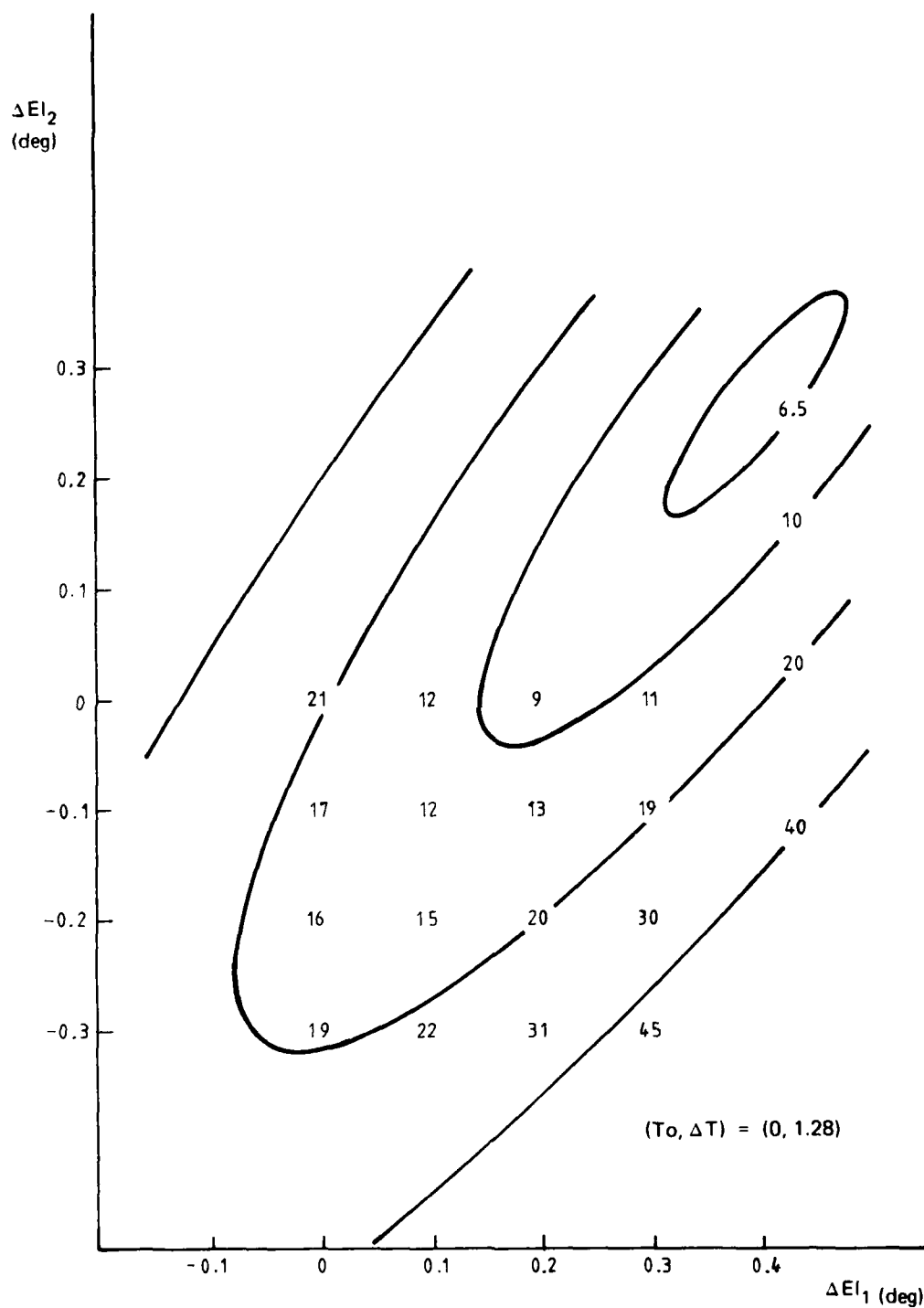
FIG. 14 (ΔEI_1, ΔEI_2) SCAN: QUADRATIC SURFACE CONTOURS

40

The value $14\cdot53$ at $(\Delta Az_1, \Delta Az_2) \equiv (+0\cdot5, 0)$ is clearly a rogue value. The corresponding entry in Table 3 shows a maximum individual error term of $3\cdot55$. By comparison with other maximum error terms well below $1\cdot0$, this suggests that convergence to the necessary accuracy was not achieved. Similar conclusions would be appropriate for the entries $(\Delta Az_1, \Delta Az_2)$ equal to $(0, +1\cdot5)$ and $(+0\cdot5, +1\cdot0)$, probably so for $(+0\cdot5, +1\cdot5)$ and $(+0\cdot5, -0\cdot5)$, and possibly so for several others.

With absolute values of the error function now around 10 and less, and a shallow surface to determine, the number of iterations needs to be increased to obtain the necessary accuracy.

TABLE 3

Results from search scan of $(\Delta Az_1, \Delta Az_2)$ at $(T_0, \Delta T, \Delta El_1, \Delta El_2) \equiv (0, 1\cdot28, 0\cdot2, 0)$

ΔAz_1 (deg)	ΔAz_2 (deg)	Sum Errors	Maximum Error Loc.	Maximum Error Value	No. of Points
$-1\cdot0$	$-0\cdot5$	$12\cdot71$	2, 15	$0\cdot61$	124
$-1\cdot0$	0	$10\cdot20$	2, 15	$0\cdot51$	124
$-1\cdot0$	$+0\cdot5$	$8\cdot34$	2, 15	$0\cdot43$	124
$-1\cdot0$	$+1\cdot0$	$7\cdot02$	2, 15	$0\cdot35$	124
$-1\cdot0$	$+1\cdot5$	$6\cdot28$	2, 15	$0\cdot28$	124
$-0\cdot5$	$-0\cdot5$	$10\cdot72$	2, 15	$0\cdot50$	124
$-0\cdot5$	0	$8\cdot81$	2, 15	$0\cdot42$	124
$-0\cdot5$	$+0\cdot5$	$7\cdot86$	1, 70	$0\cdot59$	124
$-0\cdot5$	$+1\cdot0$	$6\cdot83$	2, 15	$0\cdot27$	124
$-0\cdot5$	$+1\cdot5$	$7\cdot22$	1, 70	$0\cdot69$	124
0	$-0\cdot5$	$10\cdot65$	1, 70	$0\cdot65$	124
0	0	$9\cdot14$	1, 70	$0\cdot64$	124
0	$+0\cdot5$	$8\cdot48$	1, 70	$0\cdot53$	124
0	$+1\cdot0$	$8\cdot10$	1, 70	$0\cdot35$	124
0	$+1\cdot5$	$10\cdot97$	1, 70	$2\cdot17$	124
$+0\cdot5$	$-0\cdot5$	$11\cdot29$	1, 70	$0\cdot81$	124
$+0\cdot5$	0	$14\cdot53$	1, 70	$3\cdot55$	124
$+0\cdot5$	$+0\cdot5$	$10\cdot20$	1, 70	$0\cdot58$	124
$+0\cdot5$	$+1\cdot0$	$11\cdot45$	1, 70	$1\cdot07$	124
$+0\cdot5$	$+1\cdot5$	$12\cdot45$	1, 70	$0\cdot91$	124

Repeating the exercise, over a reduced array, but to 100 iterations, yielded the results:

ΔAz_1 \ ΔAz_2	0	$+0\cdot5$	$+1\cdot0$	$+1\cdot5$
$-1\cdot0$	$10\cdot05$	$8\cdot06$	$6\cdot66$	$5\cdot90$
$-0\cdot5$	$8\cdot52$	$7\cdot19$	$6\cdot49$	$6\cdot39$
0	$8\cdot51$	$7\cdot83$	$7\cdot76$	$8\cdot36$
$+0\cdot5$	$9\cdot95$	$9\cdot89$	$10\cdot48$	$11\cdot76$

with no value of maximum error greater than $0 \cdot 60$. Note that the incremental spacing of ΔAz_1 and ΔAz_2 is $0 \cdot 5$ deg. and that the changes in error function value are relatively small. The surface shape is very shallow. Bivariate quadratic surface contours are shown in Figure 15.

From the physical arrangement of the cameras it is to be expected that sensitivity to ΔAz_2 will be low. However, incremental adjustments of ΔAz_1 should have an effect similar to that of ΔEl_1. This is because the low sight lines from Camera 1 can be corrected, to first order, either by a positive increment ΔEl_1 (nominal value $El_8 = 0$) or by a clockwise increment of ΔAz_1 on Az_8 (nominal value $Az_8 = -81 \cdot 5$), where the relative magnitudes of ΔEl_1 to ΔAz_1 reflect the approach profile slope as seen from Camera 1.

4.6.4 (ΔEl_1, ΔAz_1) Scan

On the basis of anticipated interaction between ΔEl_1 and ΔAz_1, with an approximate approach profile slope of 1 in 6 set by the PLS, a search scan of (ΔEl_1, ΔAz_1) was made, starting at $(0, 0)$ and incrementing by $(+0 \cdot 1, -0 \cdot 5)$ degrees to 100 iterations, with the expectation of encompassing a minimum in a 4 by 4 array. The results obtained were:

ΔEl_1 \ ΔAz_1	$-1 \cdot 5$	$-1 \cdot 0$	$-0 \cdot 5$	0
0	$8 \cdot 59$	$11 \cdot 18$	$15 \cdot 21$	$20 \cdot 64$
$+0 \cdot 1$	$8 \cdot 04$	$7 \cdot 81$	$9 \cdot 08$	$11 \cdot 80$
$+0 \cdot 2$	$13 \cdot 14$	$10 \cdot 05$	$8 \cdot 52$	$8 \cdot 51$
$+0 \cdot 3$	$23 \cdot 84$	$17 \cdot 88$	$13 \cdot 53$	$10 \cdot 75$

The value $20 \cdot 64$ at $(\Delta El_1, \Delta Az_1) = (0, 0)$ at 100 iterations, when compared with the corresponding value $21 \cdot 32$ at $(\Delta El_1, \Delta El_2) = (0, 0)$ at 50 iterations in the $(\Delta El_1, \Delta El_2)$ scan, shows that the $(\Delta El_1, \Delta El_2)$ scan values (Section 4.6.2) were not fully converged at 50 iterations.

Bivariate quadratic contours appropriate to the $(\Delta El_1, \Delta Az_1)$ data above are shown in Figure 16. The strong correlation anticipated is apparent, but at a slope closer to 1 in 10 than to the 1 in 6 of the PLS. This is a reflection of the low approach path for the case being examined.

The centre of the contours is close to $(\Delta El_1, \Delta Az_1) = (0, -2 \cdot 0)$ so that the data at this stage would suggest an angular bias in the azimuth of Camera 1. Again it must be emphasised that absolute minimum has not yet been found. Also, a 2 degree error in azimuth seems inordinately large in view of the accuracy obtainable from the theodolite survey, in which measurements were taken to the nearest half minute (i.e. 2 orders better).

With respect to the reconstructed trajectory, varying the values for $(\Delta El_1, \Delta Az_1)$ along the axis of correlation (Fig. 16) has little effect. The mean approach path remains largely unchanged although the textural deviations are moved towards or away from the aiming point. Hence in drawing inferences relating to angle of approach, and approach aid guidance, the effects are negligible.

4.7 Free Search

In practice, no rigorous procedure was adopted initially for the interactive phases. Those approaches which, from the raw data, appeared to have the greatest texture (on which to achieve correlation) were processed first and the interactions exhibited in Sections 4.6.1 to 4.6.4 were quickly apparent.
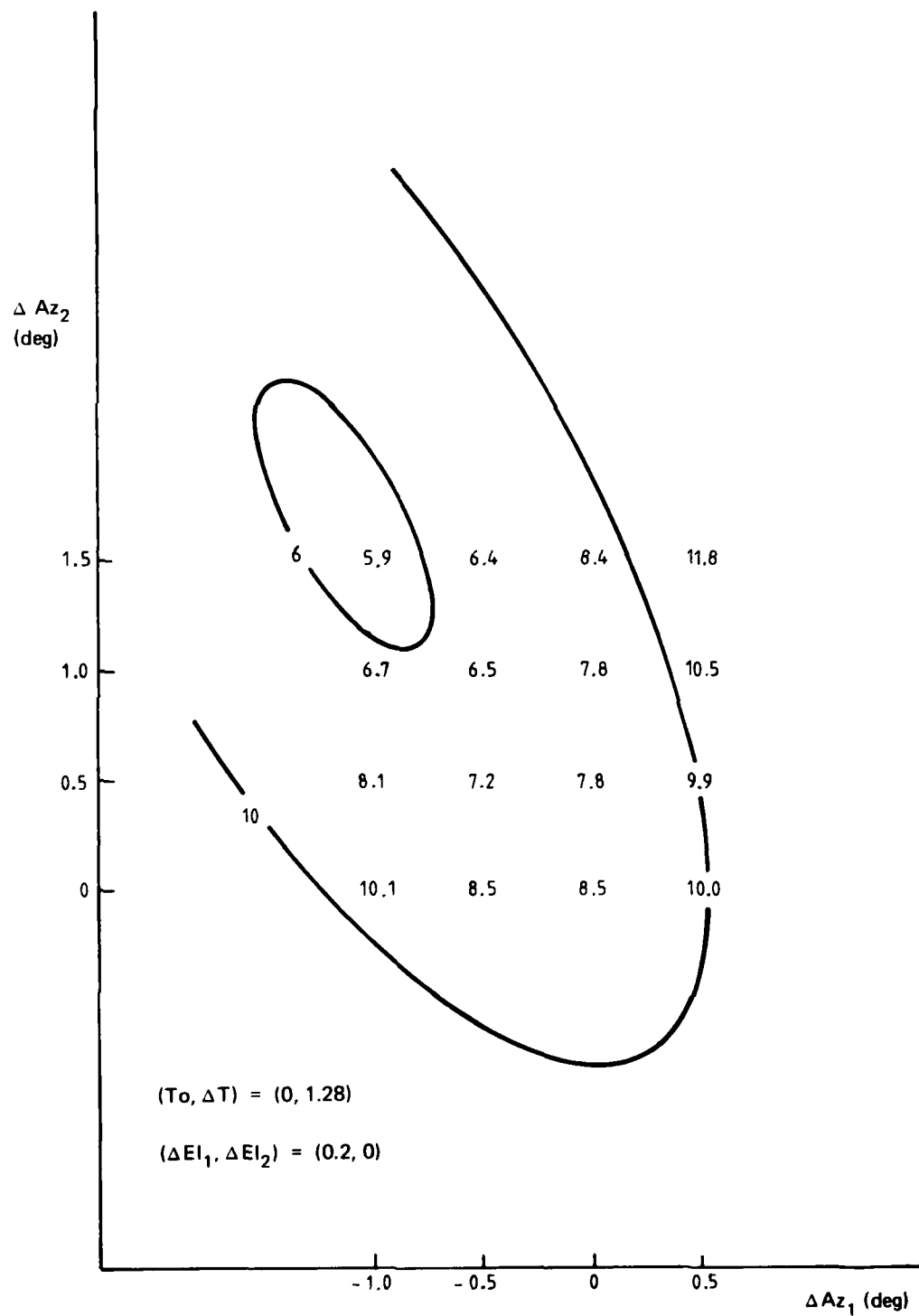
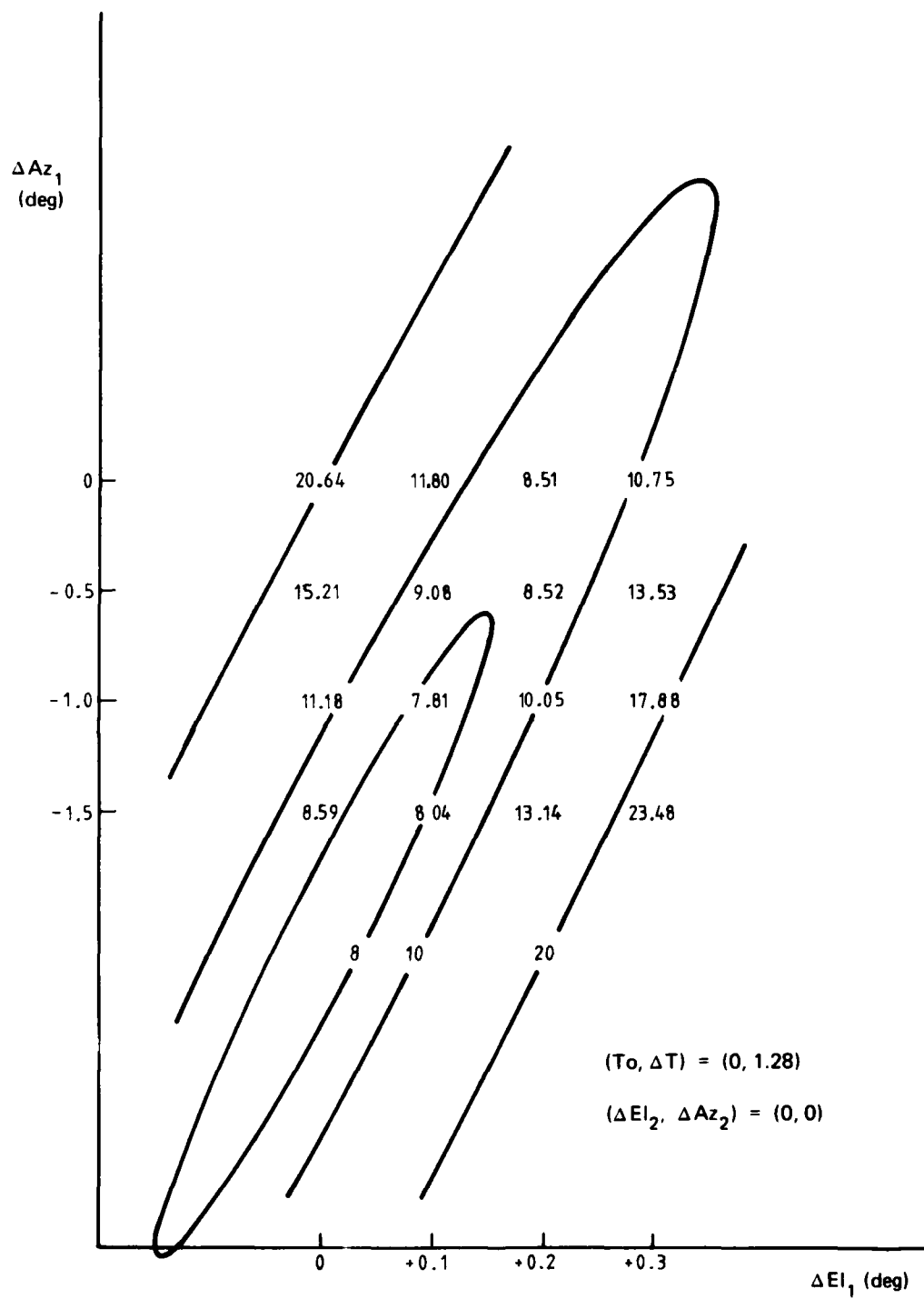FIG. 15 (ΔAz_1, ΔAz_2) SCAN: QUADRATIC SURFACE CONTOURS

43

FIG. 16 (ΔEI_1, ΔAz_1) SCAN: QUADRATIC SURFACE CONTOURS

44

Trends, that were consistent across the ensemble, were sought in order to gauge where steady bias errors existed, and where dependencies between parameters could be found, interpreted and anticipated to hold for all trajectories.

Based on the broad results described in Section 5, a free search solution, for the Rockhampton 15 trajectory data covered in detail in this section, was found for $(T_0, \Delta T, \Delta El_1) = (1 \cdot 1, 1 \cdot 27, 0 \cdot 285)$ with $(\Delta El_2, \Delta Az_1, \Delta Az_2) = (0, 0, 0)$. The error function value, summed over 123 points, was $4 \cdot 1$. Solution trajectory details etc. are given in Table 4(a),(b),(c).

4.8 Solution Data

The (x, y, z) coordinates of points on the reconstructed smoothed trajectory corresponding to the observation times of Camera 1 exposures are listed in Table 4(a). Similarly, those for Camera 2 are given in Table 4(b).

The original data values (from film reading) are also listed, together with the differences between those values and the corresponding values calculated from the smoothed trajectory coordinates. The sums of moments, to fourth power, of those differences are given in Table 4(c) for each camera. These moments provide indications of the distribution of residual errors.

From a cursory scan of the columns of differences in Table 4(a) and (b) it can be seen that the majority of values lie in the range $-0 \cdot 3$ to $+0 \cdot 3$ (mm), and that there are few long sequences of positive or negative sign that would indicate systematic errors. Thus although there may be some isolated point discrepancies, there appears to be a good match of texture between the two sets of camera data.

With respect to the isolated gross discrepancies it is revealing to review the raw data values corresponding to those difference values with magnitudes in excess of $0 \cdot 5$. Film reading errors may be inferred in many cases, and extreme sensitivity near the hover may well account for those at the end. In particular:

(a) Camera 1, Frame No. 10, $\delta\psi_1 = 0 \cdot 5601$

The value of $-123 \cdot 5$ for ψ_1 is probably in error. The sequence of first differences in the ψ_1 values suggests a more likely raw data value of $-122 \cdot 5$ viz:
listed:

$$-134 \cdot 5 \quad -130 \cdot 5 \quad -126 \cdot 5 \quad -123 \cdot 5 \quad -119 \cdot 0 \quad -115 \cdot 0 \quad 111 \cdot 5$$
$$+4 \cdot 0 \quad\quad +4 \cdot 0 \quad\quad +3 \cdot 0 \quad\quad +4 \cdot 5 \quad\quad +4 \cdot 0 \quad\quad +3 \cdot 5$$

likely:

$$-134 \cdot 5 \quad -130 \cdot 5 \quad -126 \cdot 5 \quad -122 \cdot 5 \quad -119 \cdot 0 \quad -115 \cdot 0 \quad 111 \cdot 5$$
$$+4 \cdot 0 \quad\quad +4 \cdot 0 \quad\quad +4 \cdot 0 \quad\quad +3 \cdot 5 \quad\quad +4 \cdot 0 \quad\quad +3 \cdot 5$$

(b) Camera 1, Frame No. 7, $\delta\alpha_1 = 0 \cdot 5604$
     Frame No. 8, $\delta\alpha_1 = 0 \cdot 5540$

There is no immediately obvious 'rogue' value in the sequence of values for α_1, but there are also large valued differences, $\delta\alpha_2$, at approximately the same time, viz:

Camera 2, Frame No. 5, $\delta\alpha_2 = -0 \cdot 8264$
     Frame No. 6, $\delta\alpha_2 = -0 \cdot 8826$

which point to the misreadings in the α_2 sequence, and suggest that the α_2 values for Camera 2, Frame Nos. 5 and 6 should have been $70 \cdot 5$ and $69 \cdot 0$ respectively instead of $71 \cdot 5$ and $70 \cdot 0$.

(c) Camera 2, Frame No. 29, $\delta\alpha_2 = -0 \cdot 5437$

A value $29 \cdot 5$ for α_2 is more likely than the listed value of $30 \cdot 5$.

TABLE 4(a) Reconstructed Trajectory - Camera 1 Int

CAMERA   1

Frame NO.	Time	Smoothed Point			Raw Data		Diff		
		x	y	z	AZIM	ELEV			
2	2.00	-50.486	974.370	216.575	-156.00	59.50	0		
3	3.00	-47.702	954.604	210.417	-152.00	58.50	0.0414	0	
4	4.00	-44.746	935.235	204.366	-147.50	57.70	-0.2378	0.05	
5	5.00	-41.618	916.260	198.372	-143.50	55.50	0.0058	0	
6	6.00	-38.093	897.634	192.382	-139.50	54.00	0.4.9	0.35	
7	7.00	-34.751	879.476	186.417	-134.50	52.50	-0.2	0.560	
8	8.00	-31.999	862.259	180.071	-130.50	51.00	-0.041	0.540	
9	9.00	-29.820	845.984	173.251	-126.50	49.50	-0.1619	0.43	
10	10.00	-27.917	830.518	166.049	-123.50	48.00	0.5003	0.15	
11	11.00	-25.872	815.182	159.052	-119.00	46.50	-0.1416	-0.1166	
12	12.00	-23.782	799.798	152.287	-115.00	45.00	-0.2437	-0.3523	
13	13.00	-21.807	784.630	145.576	-111.50	43.00	0.1556	-0.1026	
14	14.00	-19.954	769.540	138.854	-107.50	41.00	0.0871	0.1169	
15	15.00	-18.227	754.542	132.352	-103.50	39.00	0.0489	0.3762	
16	16.00	-16.687	740.131	126.167	-99.50	37.50	-0.0960	0.2001	
17	17.00	-15.656	726.712	120.145	-96.00	36.00	-0.0179	0.0524	
18	18.00	-14.896	714.011	114.216	-92.50	34.50	-0.1145	-0.0930	
19	19.00	-14.508	702.233	108.439	-89.50	33.00	0.0364	-0.2146	
20	20.00	-14.094	690.749	103.086	-86.50	31.50	0.1655	-0.2321	
21	21.00	-13.527	679.192	98.103	-83.00	30.00	-0.1104	-0.1591	
22	22.00	-13.063	667.766	93.270	-80.00	28.50	0.1083	-0.0550	
23	23.00	-12.623	656.421	88.639	-76.50	27.00	-0.1532	0.0950	
24	24.00	-12.411	645.478	83.939	-73.50	25.50	-0.0214	0.2088	
25	25.00	-12.040	635.062	79.449	-70.50	24.50	0.0242	-0.1386	
26	26.00	-11.371	624.975	75.314	-67.50	23.50	0.0546	-0.3994	
27	27.00	-10.776	615.307	71.404	-64.50	22.00	-0.0168	-0.1008	
28	28.00	-10.119	606.031	67.849	-61.50	21.00	-0.1666	-0.2022	
29	29.00	-9.782	597.297	64.577	-59.00	20.00	0.0027	-0.2145	
30	30.00	-9.652	588.965	61.635	-56.50	19.00	0.0473	-0.1236	
31	31.00	-9.536	580.848	59.095	-54.00	18.00	0.0502	0.0926	
32	32.00	-9.291	573.004	56.848	-51.50	17.00	0.0017	0.3935	
33	33.00	-8.951	565.513	54.893	-49.00	16.50	-0.1241	0.2836	
34	34.00	-8.536	558.264	53.166	-47.00	16.50	0.1995	-0.2583	
35	35.00	-8.199	551.100	51.562	-44.50	16.00	0.0013	-0.2605	
36	36.00	-8.004	544.041	50.048	-42.00	15.50	-0.2329	-0.2330	
37	37.00	-7.979	537.154	48.679	-40.00	15.00	-0.0266	-0.1564	
38	38.00	-8.101	530.347	47.016	-38.00	14.50	0.1506	-0.1798	
39	39.00	-8.287	523.078	45.009	-35.50	13.50	-0.0146	0.1795	
40	40.00	-8.363	514.903	43.136	-33.00	13.00	0.1447	0.0816	
41	41.00	-8.331	506.096	41.526	-30.00	12.50	0.0432	0.0705	
42	42.00	-8.151	496.570	40.300	-26.50	12.50	-0.2843	-0.3130	
43	43.00	-7.982	486.655	38.876	-23.50	12.00	0.0391	-0.2666	
44	44.00	-7.817	476.251	37.316	-20.00	11.50	0.0501	-0.2699	
45	45.00	-7.509	464.996	36.129	-16.00	11.00	-0.1140	-0.1473	
46	46.00	-7.151	452.830	35.337	-12.00	10.50	0.0623	0.1107	
47	47.00	-6.706	439.741	34.989	-7.50	10.50	0.0895	0.0224	
48	48.00	-6.200	425.745	35.024	-2.50	10.50	-0.0384	0.0670	
49	49.00	-5.538	411.175	35.290	2.50	10.50	0.0689	0.1889	
50	50.00	-4.639	396.433	35.596	8.00	11.00	-0.2318	-0.1818	
51	51.00	-3.704	381.367	35.690	13.00	11.00	0.0975	-0.1300	
52	52.00	-2.674	366.086	35.578	18.50	11.00	0.0157	-0.1556	
53	53.00	-1.724	350.268	35.250	24.00	11.00	0.1269	-0.2586	
54	54.00	-0.860	334.087	34.781	30.00	10.50	-0.1319	0.0868	
55	55.00	-0.067	317.957	34.221	35.50	10.50	0.0882	-0.1028	
56	56.00	0.655	301.723	33.548	41.50	10.50	-0.1614	-0.3349	
57	57.00	1.367	285.777	32.777	47.00	10.00	-0.0249	-0.1053	
58	58.00	2.037	270.350	31.872	52.50	9.50	-0.0877	0.0737	
59	59.00	2.724	255.311	30.818	57.50	9.50	0.1911	-0.3034	
60	60.00	3.451	240.728	29.570	63.00	8.50	-0.2170	0.2477	
61	61.00	4.196	226.523	28.102	67.50	8.00	0.2139	0.2197	
62	62.00	5.029	212.858	26.424	72.50	7.50	-0.0788	0.1154	
63	63.00	5.821	199.838	24.521	77.00	6.50	-0.1247	0.4327	
64	64.00	6.585	187.395	22.456	81.00	6.00	0.1019	0.1946	
65	65.00	7.261	175.137	20.376	85.00	5.00	0.2399	0.4540	
66	66.00	7.875	163.263	18.185	89.50	4.50	-0.2787	0.1772	
67	67.00	8.369	151.378	16.258	93.00	4.00	0.1858	-0.0043	
68	68.00	8.668	139.183	15.090	97.00	3.50	0.2400	0.0859	
69	69.00	8.798	126.805	14.529	101.50	3.50	-0.1610	-0.1162	
70	70.00	8.759	114.243	14.549	105.00	3.50	0.4828	-0.1117	

TABLE 4(b) Reconstructed Trajectory – Camera 2 data

CAMERA 2

Frame NO.	Time	Smoothed Point			Raw Data		Diffs (calc-raw)	
		x	y	z	AZIM	ELEV		
1	2.37	-49.476	967.010	214.259	-17.00	74.00	-0.1501	0.2698
2	3.64	-45.830	942.162	206.538	-16.50	73.50	0.1917	-0.0045
3	4.91	-41.907	917.952	198.910	-15.50	73.00	0.1912	-0.3376
4	6.18	-37.520	894.363	191.299	-14.00	72.00	-0.0708	-0.2586
5	7.45	-33.456	871.627	183.616	-13.00	71.50	0.1229	-0.8264
6	8.72	-30.448	850.504	175.166	-12.00	70.00	-0.0142	-0.8826
7	9.99	-27.938	830.674	166.119	-11.50	67.00	0.2087	0.1378
8	11.26	-25.351	811.193	157.250	-10.50	65.00	0.0042	0.1040
9	12.53	-22.721	791.746	148.734	-9.50	63.00	-0.1413	0.1135
10	13.80	-20.310	772.527	140.164	-9.00	61.00	0.1639	-0.0210
11	15.07	-18.120	753.529	131.900	-8.00	59.00	-0.0846	-0.1452
12	16.34	-16.273	735.458	124.084	-7.50	57.00	0.0584	-0.2567
13	17.61	-15.160	718.871	116.496	-7.00	54.50	-0.0951	0.0205
14	18.88	-14.573	703.661	109.104	-7.00	52.00	0.0302	0.1823
15	20.15	-14.024	689.014	102.306	-7.00	49.50	0.1481	0.4860
16	21.42	-13.328	674.383	96.041	-6.50	48.00	-0.1550	-0.0444
17	22.69	-12.740	659.854	90.005	-6.50	46.00	-0.0028	-0.0164
18	23.96	-12.426	645.906	84.119	-6.00	44.00	0.0185	-0.1235
19	25.23	-11.926	632.716	78.468	-6.50	41.50	0.1483	0.2919
20	26.50	-11.064	620.085	73.311	-6.00	39.50	-0.0142	0.3493
21	27.77	-10.227	608.114	68.638	-5.50	38.00	-0.1695	0.0508
22	29.04	-9.770	596.953	64.456	-5.50	36.00	-0.0186	0.4063
23	30.31	-9.595	586.425	60.799	-5.50	35.00	-0.0176	-0.0381
24	31.58	-9.403	576.247	57.752	-5.50	34.00	-0.0033	-0.2001
25	32.85	-9.000	566.630	55.179	-5.50	33.00	0.1431	-0.1548
26	34.12	-8.499	557.396	52.962	-5.00	32.00	-0.1429	0.0501
27	35.39	-8.110	548.341	50.964	-5.00	31.00	0.0112	0.3524
28	36.66	-7.975	539.532	49.232	-5.00	30.50	0.0138	0.2827
29	37.93	-8.095	530.855	47.137	-5.00	30.50	-0.1443	-0.5437
30	39.20	-8.302	521.507	44.655	-5.50	28.50	0.1292	0.3897
31	40.47	-8.361	510.844	42.347	-5.50	28.00	-0.0223	-0.0293
32	41.74	-8.187	499.067	40.674	-5.50	27.50	-0.0355	0.0006
33	43.01	-7.980	486.552	38.863	-5.50	27.00	-0.0041	-0.0475
34	44.28	-7.743	473.165	36.976	-5.50	26.00	-0.0222	0.3709
35	45.55	-7.322	458.421	35.642	-5.00	26.00	0.1101	0.2373
36	46.82	-6.792	442.144	35.033	-5.00	27.00	-0.1836	-0.2629
37	48.09	-6.144	424.473	35.030	-5.00	27.50	0.1163	0.3457
38	49.36	-5.261	405.901	35.345	-4.50	29.50	0.1271	-0.1213
39	50.63	-4.055	386.972	35.677	-3.50	31.00	-0.0345	0.1014
40	51.90	-2.770	367.640	35.598	-2.50	32.50	-0.0410	0.1604
41	53.17	-1.572	347.566	35.105	-1.50	34.00	-0.0252	0.1413
42	54.44	-0.502	326.998	34.546	-0.50	35.50	-0.0174	0.1250
43	55.71	0.441	306.355	33.752	0.50	37.00	-0.0141	0.1467
44	56.98	1.353	286.090	32.794	1.50	38.50	0.0942	0.1430
45	58.25	2.212	266.553	31.619	3.00	40.00	-0.2029	-0.0164
46	59.52	3.097	247.679	30.197	4.00	41.00	0.2141	0.0896
47	60.79	4.035	229.455	28.427	6.00	42.00	-0.0734	-0.2508
48	62.06	5.076	212.059	26.318	8.00	42.00	0.0659	-0.1792
49	63.33	6.070	195.627	23.875	10.50	41.50	-0.0437	-0.3736
50	64.60	7.000	180.001	21.206	13.00	40.00	0.1055	-0.2982
51	65.87	7.806	164.827	18.430	16.00	38.00	-0.0388	-0.3140
52	67.14	8.421	149.682	16.060	19.00	35.50	-0.0392	0.6612
53	68.41	8.742	134.130	14.793	22.00	36.00	-0.0404	1.1620
54	69.68	8.789	118.283	14.479	25.00	42.00	0.0232	-0.7804

47

TABLE 4(c) Reconstructed Trajectory - Solution data

```
SOLUTION DATA

Parameter Set
  Timing Scale Factor                      =        1.2700000
  Timing Origin                            =        1.1000000
  Perturbation of Azimuth of Camera 1      =        0.0000000
  Perturbation of Elevation of Camera 1    =        0.2850000
  Perturbation of Azimuth of Camera 2      =        0.0000000
  Perturbation of Elevation of Camera 2    =        0.0000000
  Error Weighting                          =        0.5000000

Error Data
  Sum of Errors                            =        4.1157312
  Maximum Error Location                   =        2.53
  Maximum Error Value                      =        0.3412119
  Number of Points                         =        123
  Mean Error                               =        0.0334612

Difference Moments
  Camera 1
    SUM (ELEV)      =     -0.0741920    SUM (AZIM)      =        0.6003871
    SUM (ELEV**2) =      3.8603144    SUM (AZIM**2) =      1.9690058
    SUM (ELEV**3) =      0.4464454    SUM (AZIM**3) =      0.3221048
    SUM (ELEV**4) =      0.5268412    SUM (AZIM**4) =      0.2487223
  Camera 2
    SUM (ELEV)      =      0.6448631    SUM (AZIM)      =        0.3471214
    SUM (ELEV**2) =      6.5682282    SUM (AZIM**2) =      0.6104735
    SUM (ELEV**3) =      0.2578970    SUM (AZIM**3) =      0.0203098
    SUM (ELEV**4) =      3.8134270    SUM (AZIM**4) =      0.0163171
```

(*d*) Camera 2, Frame No. 52, $\delta\alpha_2 = 0 \cdot 6612$
Frame No. 53, $\delta\alpha_2 = 1 \cdot 1620$
Frame No. 54, $\delta\alpha_2 = -0 \cdot 7804$

These correspond to points at the extreme end of the trajectory, with the helicopter initiating an overshoot and about to fly out of the field of view of Camera 2. Apart from the possibility of a misreading of the raw data, there is also extreme sensitivity in the position estimates due to the time matching between cameras in combination with the effect of short slant range from Camera 2. Further, it is probable that the smoothing process and extrapolation to the last two points is inadequate to model faithfully the actual trajectory flown. Thus no inference can be made with confidence.

The sequence of individual trajectory points corresponding to the nominal 1 second timing of camera 1 is plotted in Figures 17(*a*) and (*b*). Figure 17(*a*) shows the vertical profile, i.e. height, z, against range, y, and Figure 17(*b*) shows the plan positions, i.e. cross-range, x, against range, y.

5. RESULTS

The procedure was applied to the experimental data obtained from 14 aircraft approaches. Across the ensemble of results it was found that the values of ΔT corresponding to individual 'optimum' solutions were all close to $1 \cdot 27$ second, with well defined minima as ΔT and T_0 were varied. That result indicates, with reasonable confidence, that the camera speeds were stable and constant for all approaches. Refining ΔT to less than one hundredth of a second was judged to be unwarranted and a fixed value of $1 \cdot 27$ second was adopted for ΔT in the final reconstruction of the trajectories. Given that value for ΔT, time meshing of the data from the two cameras is then directly dependent on T_0. Resolution of T_0 to less than one tenth of a second was also judged to be unwarranted.

In general terms the individual 'optima' were found to be insensitive to ΔAz_2, as might be expected, and to indicate broadly that ΔAz_1 was near zero. This is consistent with the level of accuracy possible from the theodolite survey of the experimental site. Small value errors of the order of $0 \cdot 1$ degrees in either azimuth angle would have insignificant effects on the reconstructed approach profile. Both ΔAz_1 and ΔAz_2 were accepted as having values of zero.

The elevation values ΔEl_1 and ΔEl_2 were more equivocal. The strong interaction between these parameters, illustrated in Figure 14, results from camera/site geometry and is such that bulk correction of bias can be achieved by parametric variation of either term. However, varying ΔEl_2 around an optimum tends to produce sequences of residual differences of constant sign but of opposite signs at opposite ends of the trajectory (viz: positive at the start of the approach and negative near the hover end, or vice versa) indicating inability to effect complete removal of systematic error. Correction through ΔEl_1 was invariably more effective.

Similarly, the strong interaction between ΔEl_1 and ΔAz_1, illustrated in Figure 16, results from the approach slope and location of Camera 1, and is such that bulk correction by either parameter is possible. Across the ensemble of trajectories, individual 'optimum' solutions indicated a trend towards a zero value for ΔAz_1 but positive values for ΔEl_1. Particular trajectory solutions along the line of correlation between ΔEl_1 and ΔAz_1 have little effect on solution points *as seen from the landing aid* and therefore will not affect conclusions drawn about the sensitivity etc. of the aid. Finally it was considered that potential errors in ΔEl_1 of up to $0 \cdot 5$ degrees were feasible but that corresponding required corrections of up to 5 degrees in ΔAz_1 were unreasonable. The subjective conclusion from processing all trajectories was that the error lay in El_1 and should be corrected through ΔEl_1.

The family of results is given in Table 5 for the ensemble of 14 trajectory reconstructions with the allowable perturbations limited to T_0 and ΔEl_1, and ΔT held at $1 \cdot 27$ second. Some marginally better 'optimum' solutions were possible by variation of other parameters but, across the ensemble, there was no clear evidence that parameters other than ΔEl_1 should be varied.

The particular results given in Table 5 show a spread of values for ΔEl_1 between $0 \cdot 0$ and $0 \cdot 5$
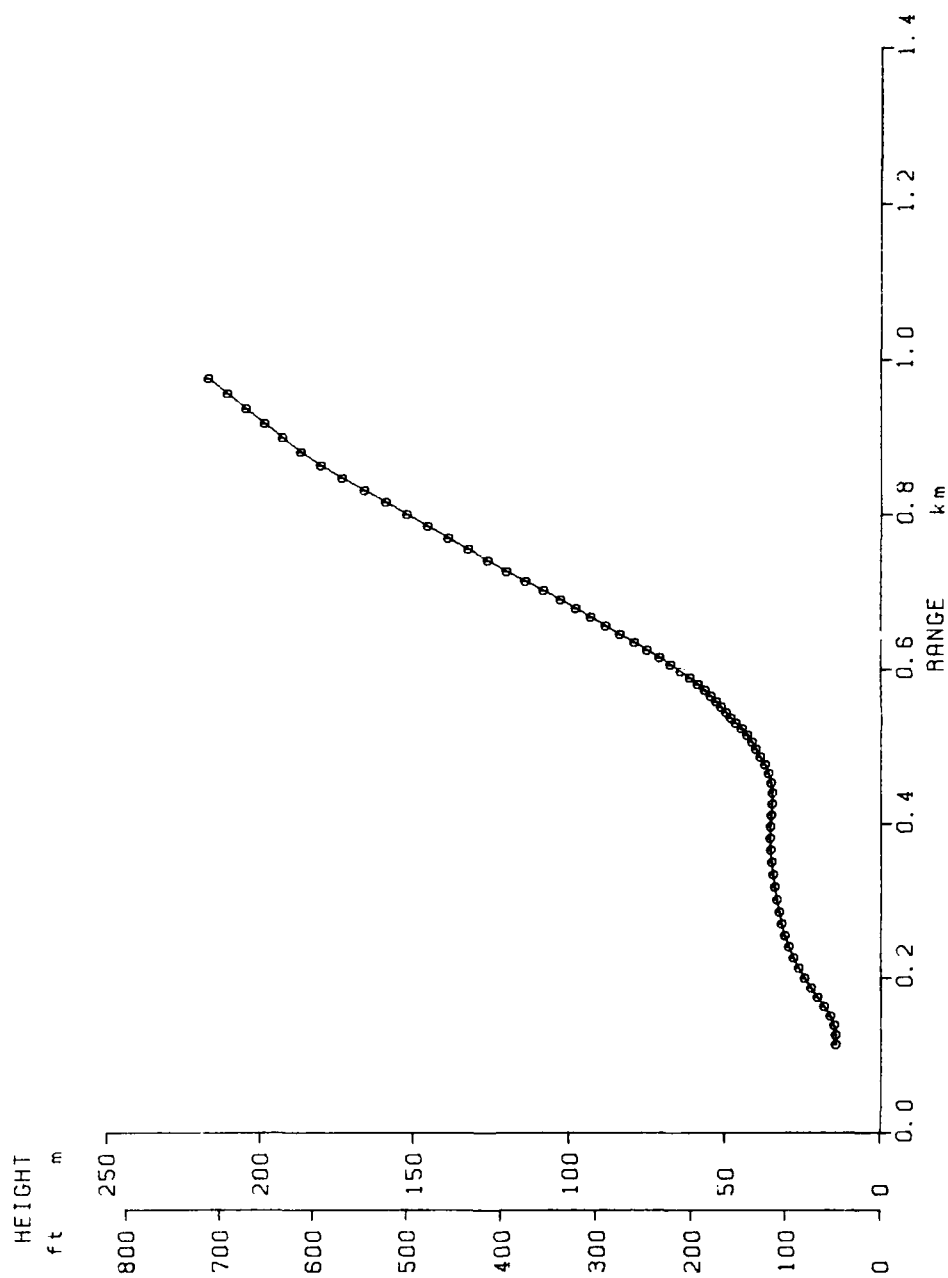
FIG. 17(a) ROCKHAMPTON 15, RECONSTRUCTED TRAJECTORY
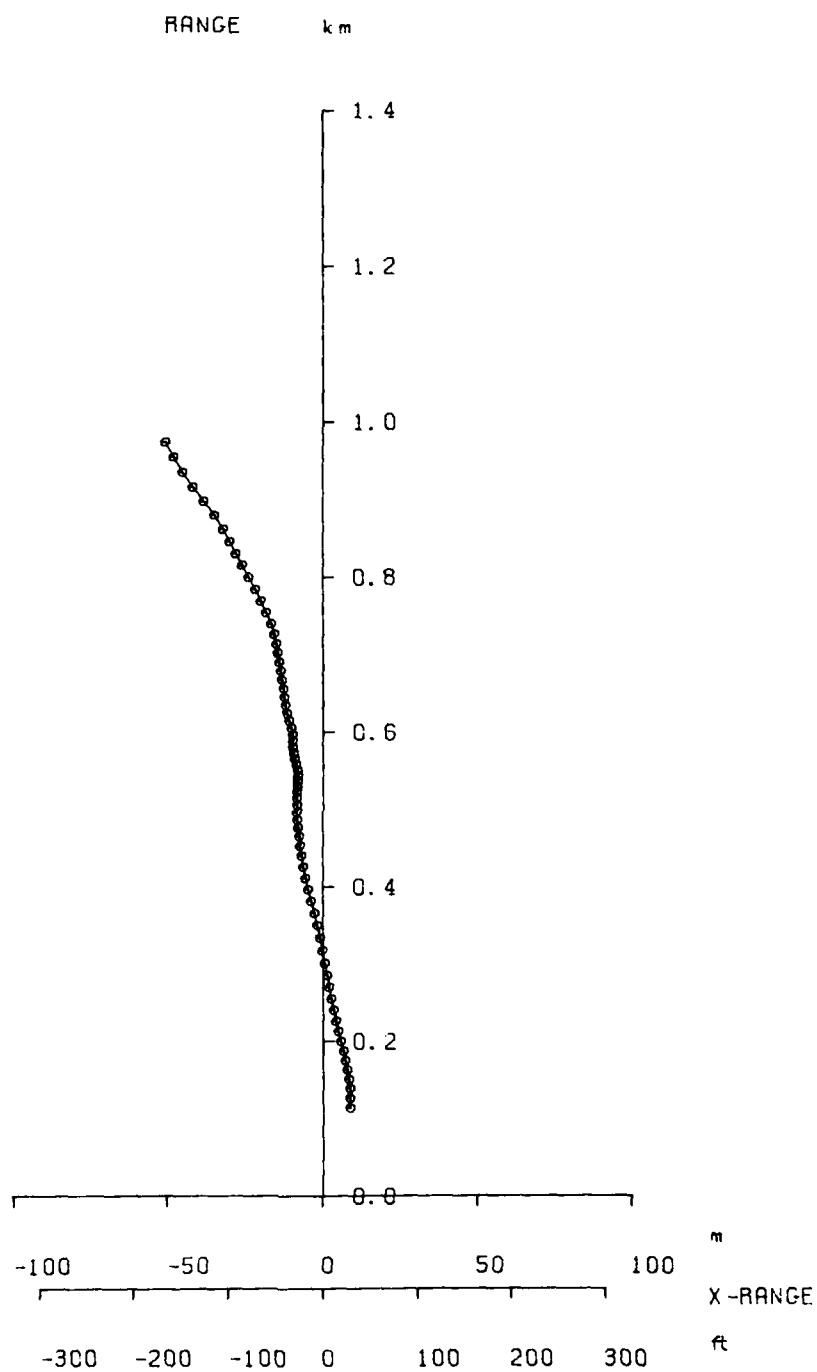HEIGHT (z) vs RANGE (y)

50

FIG. 17(b) ROCKHAMPTON 15, RECONSTRUCTED TRAJECTORY
CROSS-RANGE (x) vs RANGE (y)

51

degree. Errors of that magnitude would not have been noticeable to the camera operator and are certainly feasible. The possibility that a steady bias error was present on the elevation of Camera 1 was tested by re-running the program with a fixed value of ΔEl_1 equal to the mean of those in Table 5. The results produced error function values of sufficient magnitude for that possibility to be deemed to be invalid.

TABLE 5

Data for ensemble of 14 trajectories

Ref. No.	T_0 (second)	ΔEl_1 (deg)	Sum Errors	Number of Points
R3	−26·2	0·15	4·51	119
R5	−53·0	0·20	5·25	121
R6	·16·4	0·19	4·85	132
R8	−34·3	0·31	3·99	128
R9	−1·7	0·38	5·29	138
R12	−9·3	0·435	10·92	168
R13	3·4	0·155	5·41	133
R14	−74·5	0·43	8·33	175
R15	1·1	0·285	4·12	123
R16	−70·5	0·23	9·65	160
R17	−74·2	0·34	6·01	168
R18	−17·8	0·40	5·32	135
R19	−82·0	0·05	5·79	177
R20	−19·3	0·27	6·31	186

No cause has yet been established for the variation in El_1 although several hypotheses have been put forward. These centre on defects in the film registering mechanism of the camera, the external motor/gearbox used to reduce frame rate, or the mounting of the camera on its tripod. Similar factors of inertia and/or backlash are involved in each case, and are coupled to the stop/start action and torque drive of the electric motor. Attempts to isolate the cause have now been abandoned.

In the mid-trajectory region, at around 600 metres from each camera, an error in El_1 of 0·5 degrees corresponds to a height span of 5 metres. Resolving ΔEl_1 to 0·01 implies attempting to resolve the aircraft height to 0·1 metre. This would be unrealistic in terms of determining the trajectory, but is reasonable in terms of determining bias error in the camera when the pooling of data over 100 or more points is involved.

With respect to trajectory reconstruction, the smoothing process embedded within the iterative procedure will reduce 'noise' arising from the instrumentation process and from the true trajectory, to the extent that the smoothing model may be inadequate to represent the true trajectory. No data is available on the 'roughness' of the flight paths or conditions and it is believed that conditions were reasonably smooth. The reconstructed trajectories are therefore likely to be faithful representations of the actual flight paths. The initial objective was to resolve the flight paths to an accuracy of the order of ±1 metre, and it is believed that that has been achieved.

The full set of trajectory plots reconstructed from the Rockhampton experiment data is given in Reference 1. The computer program used was CAMCAL.FOR, written in Fortran 77 and run on the ARL VAX 11/780.

ACKNOWLEDGEMENTS

REFERENCE

1. Millar, J., and Selway, R. E. 'Performance of CH-47 (Chinook) Helicopter Pilots Using the Proportional Landing System'. ARL Systems Report (to be published).

APPENDIX 1

Straight Line Trajectory with Speed Variation

1. Problem

To find the 'best' straight line trajectory fit to a set of points (in three dimensions) where the data, although representing samples equispaced in time, do not represent equal intervals in space due to the velocity not being constant.

2. Simple Case: 3 Points

Three points define a plane; thus the problem can, without loss of generality, be reduced to one in two dimensions:
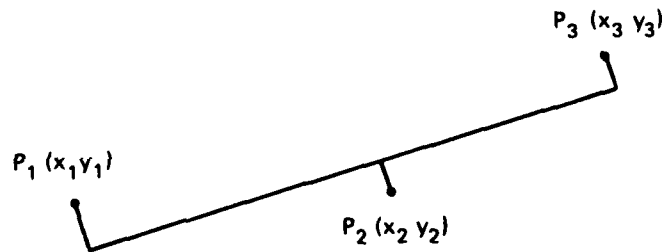
We can reasonably expect the fitted line to pass through the mean of the points, and to be aligned close to the vector direction $\hat{x}_3 - \hat{x}_1$.

Assuming a speed of u at time zero corresponding to the central point, P_2, together with constant acceleration, a, the linear distances, s, along the trajectory can be expressed as:

$$S_{-1} = S_0 - u + \tfrac{1}{2}a$$

$$S_0 = S_0$$

$$S_{+1} = S_0 + u + \tfrac{1}{2}a$$

for which the mean value S^* satisfies

$$3S^* = 3S_0 + a$$

$$S^* = S_0 + \tfrac{1}{3}a$$

and

$$S_{-1} = S^* - u + \tfrac{1}{6}a$$

$$S_0 = S^* \quad\quad - \tfrac{1}{3}a$$

$$S_{+1} = S^* + u + \tfrac{1}{6}a.$$

Assign parametric values x^*, y^*, Δx, Δy, α which together define the three fitted points as:

$$(x^* - \Delta x + \tfrac{1}{6}\alpha\Delta x, \; y^* - \Delta y + \tfrac{1}{6}a\Delta y)$$

$$(x^* \quad\quad - \tfrac{1}{3}\alpha\Delta x, \; y^* \quad\quad - \tfrac{1}{3}\alpha\Delta y)$$

$$(x^* + \Delta x + \tfrac{1}{6}\alpha\Delta x, \; y^* + \Delta y + \tfrac{1}{6}\alpha\Delta y).$$

Any such set of three points are colinear. We require to determine the values of the parameter set to satisfy the criteria for 'best' fit.

Using a 'least squares' criteria, i.e. the minimisation of an error function of the form:

$$E = \sum_i (\lambda_i - \lambda_i')^2$$

set:

$$E = (x^* - \Delta x + \tfrac{1}{6}\alpha\Delta x - x_1)^2 + (y^* - \Delta y + \tfrac{1}{6}\alpha\Delta y - y_1)^2$$
$$+ (x^* \quad - \tfrac{1}{3}\alpha\Delta x - x_2)^2 + (y^* \quad - \tfrac{1}{3}\alpha\Delta y - y_2)^2$$
$$+ (x^* + \Delta x + \tfrac{1}{6}\alpha\Delta x - x_3)^2 + (y^* + \Delta y + \tfrac{1}{6}\alpha\Delta y - y_3)^2.$$

This is in fact, the sum of the perpendicular distances from the three data points (x_i, y_i) to the line defined by the parameter set $\{x^*, y^*, \Delta x, \Delta y, \alpha\}$.

The conditions leading to a minimum value for E are given by equating to zero the derivatives of E with respect to the parameters.

$$\tfrac{1}{2}\frac{\partial E}{\partial x^*} = (x^* - \Delta x + \tfrac{1}{6}\alpha\Delta x - x_1)$$
$$+ (x^* \quad - \tfrac{1}{3}\alpha\Delta x - x_2)$$
$$+ (x^* + \Delta x + \tfrac{1}{6}\alpha\Delta x - x_3)$$
$$= 3x^* - (x_1 + x_2 + x_3).$$

Thus

$$\frac{\partial E}{\partial x^*} = 0$$

for

$$3x^* = x_1 + x_2 + x_3$$

and similarly

$$\frac{\partial E}{\partial y^*} = 0$$

for

$$3y^* = y_1 + y_2 + y_3$$

and, as expected, the fitted line passes through the mean of the data points.

$$\tfrac{1}{2}\frac{\partial E}{\partial \Delta x} = 2\Delta x - (x_3 - x_1) + \tfrac{1}{6}\alpha\{\alpha\Delta x - (x_3 - 2x_2 + x_1)\}$$

thus to first order, with α small

$$\frac{\partial E}{\partial \Delta x} = 0$$

for

$$2\Delta x \simeq (x_3 - x_1)$$

and similarly for Δy so that, as expected, the fitted line is aligned close to the vector direction $\hat{x}_3 - \hat{x}_1$.

Note also that

$$x_3 - 2x_2 + x_1 = (x_1 + x_2 + x_3) - 3x_2$$

$$= 3(x^* - x_2)$$

so that the equation $\partial E/\partial \Delta x = 0$ can be expressed as

$$2\Delta x - (x_3 - x_1) + \tfrac{1}{3}\alpha\{\alpha\Delta x - 3(x^* - x_2)\} = 0$$

and similarly for $\partial/\partial \Delta y$ and $\partial/\partial \Delta z$.

$$\tfrac{1}{2}\partial E/\partial \alpha = \tfrac{1}{3}\Delta x\{\alpha\Delta x - 3(x^* - x_2)\} + \tfrac{1}{3}\Delta y\{\alpha\Delta y - 3(y^* - y_2)\}$$

but it is not necessary that

$$\alpha\Delta x - 3(x^* - x_2) = 0 = \alpha\Delta y - 3(y^* - y_2)$$

which would imply

$$\frac{\alpha}{3} = \frac{(x^* - x_2)}{\Delta x} \simeq \frac{(y^* - y_2)}{\Delta y}$$

and thus that (x_2, y_2) lay on the fitted line. That condition would be appropriate only if the original data points were colinear.

The equation can, however, be expressed as

$$\frac{\partial E}{\partial \alpha} = \tfrac{1}{3}\alpha\{(\Delta x)^2 + (\Delta y)^2\} - \{\Delta x(x^* - x_2) + \Delta y(y^* - y_2)\}$$

so that

$$\frac{\partial E}{\partial \alpha} = 0$$

for

$$\frac{\alpha}{3} = \frac{\dfrac{\Delta x}{\sqrt{(\Delta x)^2 + (\Delta y)^2}}(x^* - x_2) + \dfrac{\Delta y}{\sqrt{(\Delta x)^2 + (\Delta y)^2}}(y^* - y_2)}{\sqrt{(\Delta x)^2 + (\Delta y)^2}}$$

$$= \frac{l(x^* - x_2) + m(y^* - y_2)}{|\Delta s|}$$

Thus the numerator is the length of the projection (component) of the vector $\hat{x}^* - \hat{x}_2$ in the direction $(\Delta x, \Delta y)$ which has the direction cosines (l, m) of the fitted line. α is thus directly related to the ratio of the magnitude of the vector projection to the magnitude of Δs.

With a six parameter set (using x^*, y^*, Δx, Δy, α_x, α_y) an exact fit is obtained which separates the x and y variables completely, giving

$$3x^* = (x_1 + x_2 + x_3) \qquad\qquad 3y^* = (y_1 + y_2 + y_3)$$

$$2\Delta x = (x_3 - x_1) \qquad\qquad 2\Delta y = (y_3 - y_1)$$

$$\alpha_x \Delta x = 3(x^* - x_2) \qquad\qquad \alpha_y \Delta y = 3(y^* - y_2).$$

Note that $\alpha_x \Delta x$ is a measure of the acceleration component in the x direction, and $\alpha_y \Delta y$ that of the component in the y direction. Thus $\hat{x}^* - \hat{x}_2$ is a measure of the two-dimensional acceleration vector.

In fact

$$\hat{a} = \frac{3(\hat{x}^* - \hat{x}_2)}{|\Delta s|}.$$

The straight line approximation, using a common value for α in both the x and y directions, is one which uses that component of the acceleration vector which is in the direction of the fitted line.

3. General Case: N Points, N Odd

$$w_n = w_0 + n\Delta w + \tfrac{1}{2}(n^2)\alpha\Delta w \qquad w = x, y, z$$

$$\sum_n w_n = w_0 \sum_n 1 + \Delta w \sum_n n + \tfrac{1}{2}\alpha\Delta w \sum_n n^2$$

$$n = -m, \ldots -1, 0, 1, \ldots m$$

$$\text{put} \sum_n 1 = N_0 = 2m + 1$$

$$\sum_n n = N_1 = 0$$

$$\sum_n n^2 = N_2 = 2\sum_{k=1}^{m} k^2$$

$$\sum_n n^3 = N_3 = 0$$

$$\sum_n n^4 = N_4 = 2\sum_{k=1}^{m} k^4$$

N_0 sequence: 1, 3, 5, 7, 9, . . .

N_2 sequence: 0, 2, 10, 28, 60, . . .

N_4 sequence: 0, 2, 34, 196, 708, . . .

$$\sum_n w_n = N_0 \, w^*$$

$$= N_0 \, w_0 + \tfrac{1}{2} N_2 \alpha \Delta w$$

so that

$$w_0 = w^* - \tfrac{1}{2} \frac{N_2}{N_0} \alpha \Delta w$$

and

$$w_n = w^* + n\Delta w + \tfrac{1}{2} \alpha \Delta w \left(n^2 - \frac{N_2}{N_0} \right)$$

giving

$$E = \sum_{w,\,n} \left\{ w^* + n\Delta w + \tfrac{1}{2} \alpha \Delta w \left(n^2 - \frac{N_2}{N_0} \right) - w_n \right\}^2 \qquad w = x,\, y,\, z.$$

The minimum value of E is given by the simultaneous solution of the equations resulting from differentiation with respect to the parameter set $\{x^*, \, y^*, \, z^*, \, \Delta x, \, \Delta y, \, \Delta z, \, \alpha\}$.

Differentiating with respect to x^*:

$$\tfrac{1}{2} \frac{\partial E}{\partial x^*} = \sum_n \left\{ x^* + n\Delta x + \tfrac{1}{2} \alpha \Delta x \left(n^2 - \frac{N_2}{N_0} \right) - x_n \right\}$$

$$= x^* \sum_n 1 + \Delta x \sum_n n + \tfrac{1}{2} \alpha \Delta x \left(\sum_n n^2 - \frac{N_2}{N_0} \sum_n 1 \right) - \sum_n x_n$$

$$= x^* N_0 + \Delta x N_1 + \tfrac{1}{2} \alpha \Delta x (N_2 - N_2) - \sum_n x_n$$

$$= N_0 x^* - \sum_n x_n.$$

Hence

$$\frac{\partial E}{\partial x^*} = 0 \text{ for } N_0 x^* = \sum_n x_n$$

similarly

$$\frac{\partial E}{\partial y^*} = 0 \text{ for } N_0 y^* = \sum_n y_n$$

and

$$\frac{\partial E}{\partial z^*} = 0 \text{ for } N_0 z^* = \sum_n z_n.$$

Differentiating with respect to Δx:

$$\tfrac{1}{2} \frac{\partial E}{\partial \Delta x} = \sum_n \left\{ x^* + n\Delta x + \tfrac{1}{2} \alpha \Delta x \left(n^2 - \frac{N_2}{N_0} \right) - x_n \right\} \left\{ n + \tfrac{1}{2} \alpha \left(n^2 - \frac{N_2}{N_0} \right) \right\}$$

which, in similar fashion, reduces to

$$\tfrac{1}{2}\frac{\partial E}{\partial \Delta x} = N_2 \Delta x - \sum_n n x_n + \tfrac{1}{4}\alpha^2 \Delta x \left\{ N_4 - \frac{N_2{}^2}{N_0} \right\} - \tfrac{1}{2}\alpha \sum_n \left(n^2 - \frac{N_2}{N_0} \right) x.$$

For $N = 3$ as previously

$$\tfrac{1}{2}\frac{\partial E}{\partial \Delta x} = 2\Delta x - (x_3 - x_1) + \tfrac{1}{4}\alpha^2 \Delta x \{2 - \tfrac{4}{3}\} - \tfrac{1}{2}\alpha \{\tfrac{1}{3}x_3 - \tfrac{2}{3}x_2 + \tfrac{1}{3}x_1\}$$

$$= 2\Delta x - (x_3 - x_1) + \tfrac{1}{6}\alpha^2 \Delta x - \tfrac{1}{6}\alpha \{x_3 - 2x_2 + x_1\}.$$

For $N = 5$

$$\tfrac{1}{2}\frac{\partial E}{\partial \Delta x} = 10\Delta x - (2x_5 + x_4 - x_2 - 2x_1) + \tfrac{1}{4}\alpha^2 \Delta x \{34 - \tfrac{100}{5}\} - \tfrac{1}{2}\alpha \{2x_5 - x_4 - 2x_3 - x_2 + 2x_1\}$$

$$= 10\Delta x - (2x_5 + x_4 - x_2 - 2x_1) + \tfrac{7}{2}\alpha^2 \Delta x - \tfrac{1}{2}\alpha \{2x_5 - x_4 - 2x_3 - x_2 + 2x_1\}$$

and similarly for

$$\frac{\partial E}{\partial \Delta y} \quad \text{and} \quad \frac{\partial E}{\partial \Delta z}.$$

Differentiating with respect to α:

$$\tfrac{1}{2}\frac{\partial E}{\partial \alpha} = \sum_n \left\{ x^* + n\Delta x + \tfrac{1}{2}\alpha \Delta x \left(n^2 - \frac{N_2}{N_0} \right) - x_n \right\} \left\{ \tfrac{1}{2}\Delta x \left(n^2 - \frac{N_2}{N_0} \right) \right\}$$

$$+ \sum_n \left\{ y^* + n\Delta y + \tfrac{1}{2}\alpha \Delta y \left(n^2 - \frac{N_2}{N_0} \right) - y_n \right\} \left\{ \tfrac{1}{2}\Delta y \left(n^2 - \frac{N_2}{N_0} \right) \right\}$$

$$+ \sum_n \left\{ z^* + n\Delta z + \tfrac{1}{2}\alpha \Delta z \left(n^2 - \frac{N_2}{N_0} \right) - z_n \right\} \left\{ \tfrac{1}{2}\Delta z \left(n^2 - \frac{N_2}{N_0} \right) \right\}$$

which reduces to

$$\tfrac{1}{2}\frac{\partial E}{\partial \alpha} = \Delta x \left[\tfrac{1}{4}\alpha \Delta x \left\{ N_4 - \frac{N_2{}^2}{N_0} \right\} - \tfrac{1}{2}\sum_n \left\{ \left(n^2 - \frac{N_2}{N_0} \right) x_n \right\} \right]$$

$$+ \Delta y \left[\tfrac{1}{4}\alpha \Delta y \left\{ N_4 - \frac{N_2{}^2}{N_0} \right\} - \tfrac{1}{2}\sum_n \left\{ \left(n^2 - \frac{N_2}{N_0} \right) y_n \right\} \right]$$

$$+ \Delta z \left[\tfrac{1}{4}\alpha \Delta z \left\{ N_4 - \frac{N_2{}^2}{N_0} \right\} - \tfrac{1}{2}\sum_n \left\{ \left(n^2 - \frac{N_2}{N_0} \right) z_n \right\} \right].$$

For $N = 3$

$$\tfrac{1}{2}\frac{\partial E}{\partial \alpha} = \Delta x [\tfrac{1}{6}\alpha \Delta x - \tfrac{1}{6}(x_3 - 2x_2 + x_1)]$$

$$+ \Delta y [\tfrac{1}{6}\alpha \Delta y - \tfrac{1}{6}(y_3 - 2y_2 + y_1)]$$

$$+ \Delta z [\tfrac{1}{6}\alpha \Delta z - \tfrac{1}{6}(z_3 - 2z_3 + z_1)].$$

For $N = 5$

$$\frac{1}{2}\frac{\partial E}{\partial \alpha} = \Delta x[\tfrac{7}{2}\alpha\Delta x - \tfrac{1}{2}(2x_5 - x_4 - 2x_3 - x_2 + 2x_1)]$$
$$+ \Delta y[\tfrac{7}{2}\alpha\Delta y - \tfrac{1}{2}(2y_5 - y_4 - 2y_3 - y_2 + 2y_1)]$$
$$+ \Delta z[\tfrac{7}{2}\alpha\Delta z - \tfrac{1}{2}(2z_5 - z_4 - 2z_3 - z_2 + 2z_1)].$$

Summarising the 5 point case:

$$x^* = \tfrac{1}{5}(x_5 + x_4 + x_3 + x_2 + x_1)$$

and similarly for y^* and z^*,

$$\Delta x = \frac{\{2(2x_5 + x_4 - x_2 - 2x_1) + \alpha(2x_5 - x_4 - 2x_3 - x_2 + 2x_1)\}}{(20 + 7\alpha^2)}$$

and similarly for Δy and Δz,

$$\alpha = \left[\frac{\Delta x(2x_5 - x_4 - 2x_3 - x_2 + 2x_1) + \Delta y(2y_5 - y_4 - 2y_3 - y_2 + 2y_1) + \Delta z(2z_5 - z_4 - 2z_3 - z_2 + 2z_1)}{7\{(\Delta x)^2 + (\Delta y)^2 + (\Delta z)^2\}}\right].$$

The combinations

$$(2x_5 + x_4 - x_2 - 2x_1)$$

and

$$(2x_5 - x_4 - 2x_3 - x_2 + 2x_1)$$

may be regarded as higher order estimates of velocity and acceleration components, e.g.

$$2x_5 + x_4 - x_2 - 2x_1 = 2(x_5 - x_4) + 3(x_4 - x_3) + 3(x_3 - x_2) + 2(x_2 - x_1)$$
$$\simeq 10\,\Delta x$$

$$2x_5 - x_4 - 2x_3 - x_2 + 2x_1 = 2(x_5 - 2x_4 + x_3) + 3(x_4 - 2x_3 + x_2) + 2(x_3 - 2x_2 + x_1)$$
$$\simeq 7\alpha\Delta x.$$

The equations for Δx, Δy, Δz, α are interdependent and non-linear, but amenable to initial approximation and simple iterative convergence.

APPENDIX 2

Equations for Central Plane Projections

1. Sight Line

The sight lines from Camera 1 are implicitly defined by the raw data pairs (ψ_{1j}, α_{1j}) together with the location and orientation parameters for Camera 1.

The transforms from camera space to real world are given, without subscript j, by:

$$(\psi_1{}^2 + \alpha_1{}^2)^{1/2} = \rho_1$$

$$\tan^{-1}\{\rho_1/456\} = \theta_1$$

$$2 \cdot 1\,\theta_1 = \theta_1'$$

$$\tan \theta_1' = \rho_1' \qquad \text{i.e. } \tan^{-1}\{\rho_1'/1\} = \theta_1'$$

so that, in real world coordinates but in camera axes, the point Q on the sight line at range R from Camera 1 is given by

$$Q_{x1} = R\psi_1\rho_1'/\rho_1$$

$$Q_{y1} = R\rho_1'/\rho_1$$

$$Q_{z1} = R\alpha_1\rho_1'/\rho_1$$

2. Intersection with Central Plane

Rotating to the orientation of the common frame

$$[Q_0] = [R(Az_1)]^T[R(El_1)]^T[Q_1]$$

and translating to the common origin

$$Q_x = X_1 + Q_{x0}$$

$$Q_y = Y_1 + Q_{y0}$$

$$Q_z = Z_1 + Q_{z0}$$

But Q_{x0}, Q_{y0} and Q_{z0} are the vector components corresponding to vector length R along the sight line, where R can be chosen arbitrarily. Setting R equal to 1000 (say) initially, and then rescaling the components at this stage such that

$$Q_x = 0$$

$$Q_{x0} = -X_1$$

will fix the point Q on the central plane and give the corresponding y and z values as:

$$Q_y = Y_1 - Q_{y0}/X_1$$

$$Q_z = Z_1 - Q_{z0}/X_1$$

3. Inferred Elevation

Because, by definition, Camera 2 is located at the origin of, and aligned with, the common reference frame, the inferred elevation value (in mm), appropriate to data scalings for Camera 2, results from:

$$\tan^{-1}\{Q_z/Q_y\} = \theta_2'$$

$$\theta_2'/1 \cdot 35 = \theta_2$$

$$456 \tan \theta_2 = {}_2v_1$$

where ${}_2v_{1j}$ is the inferred data domain value equivalent to raw data values α_{2k}.

DISTRIBUTION

AUSTRALIA

DEPARTMENT OF DEFENCE

Central Office

Chief Defence Scientist
Deputy Chief Defence Scientist
Superintendent, Science and Program Administration
Controller, External Relations, Projects and Analytical Studies
} (1 copy)
Defence Science Advisor (U.K.) (Doc. Data sheet only)
Counsellor, Defence Science (U.S.A.) (Doc. Data sheet only)
Defence Science Representative (Bangkok)
Defence Central Library
Document Exchange Centre, D.I.S.B. (18 copies)
Joint Intelligence Organisation
Librarian H Block, Victoria Barracks, Melbourne
Director General—Army Development (NSO) (4 copies)

Aeronautical Research Laboratories

Director
Library
Superintendent—Systems
Divisional File—Systems
Principal Officer Human Factors Group
Authors: A. Ross
        L. Mockridge
        D. Drumm
J. Millar

Materials Research Laboratories

Director/Library

Defence Research Centre

Library

Navy Office

Navy Scientific Adviser
Director of Operational Analysis—Navy

Army Office

Scientific Adviser—Army
Director of Operational Analysis—Army

Air Force Office

Air Force Scientific Adviser
Aircraft Research and Development Unit
  Scientific Flight Group
  Library
Director of Operational Analysis—Air Force
Directorate of Operational Requirements B—Air Force (ORHEL)

DEPARTMENT OF AVIATION

Library

CANADA

NRC, Aeronautical & Mechanical Engineering Library

Universities and Colleges

Toronto, Institute for Aerospace Studies

UNITED KINGDOM

Royal Aircraft Establishment
  Bedford, Library
  Farnborough, Library

UNITED STATES OF AMERICA

Department of the Air Force, Dr H. J. Clark
FAA, Dr H. W. Mertons
NASA Scientific and Technical Information Facility
NASA Langley Research Center

Universities and Colleges

Ohio State, Dr R. S. Jensen

SPARES (10 copies)

TOTAL (67 copies)

1. a. AR No. AR–003–969	1. b. Establishment No. ARL–SYS–R–34		2. Document Date October 1984	3. Task No. AIR 81/101
4. Title An Optimisation Method for Reconstruction of Flight Path Trajectories from Non-Synchronous Time-Sampled Observations by Two Cine Cameras			5. Security a. document Unclassified	6. No. Pages 53
			b. title c. abstract U. U.	7. No. Refs 1
8. Author(s) A. Ross, L. Mockridge, D. Drumm			9. Downgrading Instructions —	
10. Corporate Author and Address Aeronautical Research Laboratories, P.O. Box 4331, Melbourne, Victoria, 3001			11. Authority (as appropriate) a. Sponsor c. Downgrading b. Security d. Approval a) Air Force Office	
12. Secondary Distribution (of this document) Approved for public release Overseas enquirers outside stated limitations should be referred through ASDIS, Defence Information Services Branch, Department of Defence, Campbell Park, CANBERRA, ACT, 2601.				
13. a. This document may be ANNOUNCED in catalogues and awareness services available to . . . No limitations				
13. b. Citation for other purposes (i.e, casual announcement) may be (select) unrestricted (or) as for 13 a.				
14. Descriptors Optimization ; Least squares ; Trajectories Flight paths Landing aids			15. COSATI Group 12010 14070	

16. Abstract

Helicopter flight path trajectories in approach to a tactical landing aid were monitored, ad hoc, by two cine cameras. Post-trial trajectory reconstruction using simple triangulation methods was confounded by the presence of an unknown bias error in the orientation of one camera, and by non-synchronous camera timing. The report describes the concept, formulation and implementation of an optimisation method which pools all data for a trajectory, permits extraction of bias terms, and yields a complete trajectory smoothed in space and time.

16. Abstract *(Contd)*		

17. Imprint

Aeronautical Research Laboratories, Melbourne

18. Document Series and Number	19. Cost Code	20. Type of Report and Period Covered
Systems Report 34	732260	

21. Computer Programs Used

22. Establishment File Ref(s)

END

DATE
FILMED

2 -86

DTIC